UNLV Retrospective Theses & Dissertations

1-1-2006

Adaptive design of delta sigma modulators

Gregory Kenneth Lull
University of Nevada, Las Vegas

Follow this and additional works at: https://digitalscholarship.unlv.edu/rtds

Repository Citation

Lull, Gregory Kenneth, "Adaptive design of delta sigma modulators" (2006). *UNLV Retrospective Theses & Dissertations*. 2064.
http://dx.doi.org/10.25669/ywoc-v3il

This Thesis is protected by copyright and/or related rights. It has been brought to you by Digital Scholarship@UNLV with permission from the rights-holder(s). You are free to use this Thesis in any way that is permitted by the copyright and related rights legislation that applies to your use. For other uses you need to obtain permission from the rights-holder(s) directly, unless additional rights are indicated by a Creative Commons license in the record and/or on the work itself.

This Thesis has been accepted for inclusion in UNLV Retrospective Theses & Dissertations by an authorized administrator of Digital Scholarship@UNLV. For more information, please contact digitalscholarship@unlv.edu.

ADAPTIVE DESIGN OF DELTA SIGMA MODULATORS

by

Gregory Kenneth Lull

Bachelor of Science, Electrical Engineering
University of Nevada, Las Vegas
2002

A thesis submitted in partial fulfillment
of the requirements for the

Master of Science Degree in Electrical Engineering
Department of Electrical and Computer Engineering
Howard Huges College of Engineering

Graduate College,
University of Nevada, Las Vegas
December 2006

Reproduced with permission of the copyright owner. Further reproduction prohibited without permission.

UMI Number: 1441721

INFORMATION TO USERS

The quality of this reproduction is dependent upon the quality of the copy submitted. Broken or indistinct print, colored or poor quality illustrations and photographs, print bleed-through, substandard margins, and improper alignment can adversely affect reproduction.

In the unlikely event that the author did not send a complete manuscript and there are missing pages, these will be noted. Also, if unauthorized copyright material had to be removed, a note will indicate the deletion.

UMI®

UMI Microform 1441721
Copyright 2007 by ProQuest Information and Learning Company.
All rights reserved. This microform edition is protected against
unauthorized copying under Title 17, United States Code.

ProQuest Information and Learning Company
300 North Zeeb Road
P.O. Box 1346
Ann Arbor, MI 48106-1346

Reproduced with permission of the copyright owner. Further reproduction prohibited without permission.

Copyright by Gregory Kenneth Lull 2007
All Rights Reserved

Reproduced with permission of the copyright owner. Further reproduction prohibited without permission.

UNLV
UNIVERSITY OF NEVADA LAS VEGAS

Thesis Approval
The Graduate College
University of Nevada, Las Vegas

November 14, 2006

The Thesis prepared by

Greg Lull

Entitled

"Adaptive Design of Delta Sigma Modulators"

is approved in partial fulfillment of the requirements for the degree of

Master of Science in Electrical Engineering

Examination Committee Chair

Dean of the Graduate College

Examination Committee Member

Examination Committee Member

Graduate College Faculty Representative

Reproduced with permission of the copyright owner. Further reproduction prohibited without permission.

ABSTRACT

Adaptive Design of Delta Sigma Modulators

by

Gregory Kenneth Lull

Dr. Peter Stubberud, Examination Committee Chair
Professor of Electrical Engineering
University of Nevada, Las Vegas

In this thesis, a genetic algorithm based on differential evolution (DE) is used to generate delta sigma modulator (DSM) noise transfer functions (NTFs). These NTFs outperform those generated by an iterative approach described by Schreier and implemented in the delsig Matlab toolbox. Several lowpass and bandpass DSMs, as well as DSM's designed specifically for and very low intermediate frequency (VLIF) receivers are designed using the algorithm developed in this thesis and compared to designs made using the delsig toolbox. The NTFs designed using the DE algorithm always have a higher dynamic range and signal to noise ratio than those designed using the delsig toolbox.

Reproduced with permission of the copyright owner. Further reproduction prohibited without permission.

TABLE OF CONTENTS

ABSTRACT iii

ACKNOWLEDGEMENTS vi

CHAPTER 1 INTRODUCTION 1

CHAPTER 2 REVIEW OF RELATED LITERATURE 4
  2.1 Tuned Radio Frequency Receiver 5
    2.1.2 Super Heterodyne Receiver 6
    2.1.3 Zero Intermediate Frequency (ZIF) and Very Low Intermediate Frequency (VLIF) 7
    2.1.4 Complex IF Receivers and Quadrature Signals 8
  2.2 Analog to Digital Converters 9
    2.2.1 Parallel ADCs 9
    2.2.3 Bandpass DSM 26
    2.2.4 DSM Design 27
  2.3 Adaptive Algorithms 28
    2.3.1 Learning Curves and Convergence 28
    2.3.2 Errors in Convergence 29
    2.3.3 LMS Adaptation and the Equation Error Method 30
    2.3.4 Genetic Algorithms 30

CHAPTER 3 ADAPTIVE DESIGN METHODOLOGY 34
  3.1 DSM Design using Differential Evolution 34
  3.1.1 Population Vector and Cost Function 34
  3.2 Delsig Designs 36
    3.2.1 Optimal Bandpass Designs 37

CHAPTER 4 ADAPTIVE DESIGN METHODOLOGY 38
  4.1 Design and Test Procedures 38
    4.2 Low Pass DSM Results 39
    4.2.1 Results for Second Order LPDSM 40
    4.2.2 Results for an Eight Order LPDSM 42
    4.2.3 Comparison of DR and SQNR for Delsig and DE LPDSM NTFs 44
    4.3 VLIF DSM Results 47
    4.3.1 Analysis of Second order VLIF DSM 48
    4.3.2 Comparison of fourth order VLIF DSM 49

Reproduced with permission of the copyright owner. Further reproduction prohibited without permission.

4.3.3 Comparison of DR and SQNR for Delsig and DE VLIF DSM NTFs...... 51
4.4 Bandpass DSMs........ 54
4.4.1 Comparison of Fourth Order BPDSM........ 55
4.4.2 Comparison of DR and SQNR for Delsig and DE BPDSM NTFs........... 57

CHAPTER 5 CONCLUSIONS........ 60

REFERENCES........ 62

VITA........ 64

Reproduced with permission of the copyright owner. Further reproduction prohibited without permission.

ACKNOWLEDGEMENTS

Completion of this thesis almost didn't happen. All too many graduate students finish coursework and label themselves as an "all but thesis" or "all but dissertation" graduate student. I would like to thank my advisor, Dr. Stubberud, for giving me a much needed pep talk during the last summer before my defense. I would have quit without that encouragement. He was quite correct when he told me "when you think you're about 80% done, you've only completed 20% of the work, and when you finally think you're 20% done, you've actually completed 80% of the work". That was certainly true in my case.

Additionally, I would like to thank my first employer out of undergrad, H. Del Anderson. He always encouraged me to fulfill my potential and continue my studies, even though it wasn't in his best interests to do so. Without his guidance I may not have returned for a graduate degree.

Finally, the stress associated with my degree certainly made me a less than ideal companion at times, but my fiancée, Allison, continually gave me support and understanding throughout the process. Without her encouragement I would have lost focus long ago and been doomed to be one of the many "all but thesis" graduate students. It is to her, with love and gratitude, that I dedicate the following pages.

Reproduced with permission of the copyright owner. Further reproduction prohibited without permission.

CHAPTER 1

INTRODUCTION

Digital radios which use digital signals to transmit information have revolutionized radio communications by eliminating most of the noise added to information signals during their transmission and reception. Digital radios are often implemented with software defined radio which uses software to modulate and demodulate transmitted signals. As a result, software defined digital radios can switch between different modulation protocols on the fly, and thus, these types of radios can use the same hardware to transmit and receive many different types of transmissions.

Digital radio receiver architectures such as the zero intermediate frequency (IF) (ZIF) receiver and the very low IF (VLIF) receivers use analog to digital converters (ADCs) to convert transmitted signals into digital signals which can be demodulated using a software defined radio. Unlike superheterodyne architectures that perform channel filtering and automatic gain control (AGC) after the first down conversion and digitize the received signal after a second down conversion, ZIF and VLIF architectures digitize the received signal after a single down conversion and perform AGC and channel filtering digitally. In ZIF and VLIF architectures, the ADCs, which digitize the receiver's ZIF and VLIF signals, must have a larger dynamic range and better linearity than ADCs in superheterodyne receivers. Also, because ZIF and VLIF receiver architectures

Reproduced with permission of the copyright owner. Further reproduction prohibited without permission.

typically provide little or no filtering in front of their ADCs, their ADCs need to provide their own anti-aliasing filters, and therefore, typically sample at higher rates than ADCs in superheterodyne receivers. Because delta sigma modulators (DSMs) can be designed to have large dynamic ranges, sample at very high rates, provide inherent anti-aliasing filtering, and are smaller and consume less power than many other ADC architectures with similar specifications, DSMs are a natural choice for ADCs in ZIF and VLIF receivers.

A DSM can be described by its signal transfer function (STF) and noise transfer function (NTF). A DSM's STF is the transfer function between the DSM's input and output. A DSM's STF is often designed to be an anti-aliasing filter that passes in-band signals and attenuates signals that can alias into in-band signals. The DSM's NTF is the transfer function between the DSM's quantizer and the DSM's output, and it shapes the DSM's quantization noise so that it is minimal in the signal band. Figure 1 shows an example of a STF and a NTF for a 2nd order lowpass DSM where $STF(z) = z^{-2}$ and $NTF(z) = (1 - z^{-1})^2$. As shown in Figure 1, the STF passes low in-band frequencies and attenuates higher frequencies whereas the NTF attenuates the quantization noise at the low inband frequencies.

DSM's NTFs are typically designed using traditional highpass filters such as Butterworth and Chebychev filters. However, for VLIF receiver architectures, a DSM's NTF is only required to suppress quantization noise within the signal band, which is centered at the low IF frequency. Although a traditional notch filter could be used, a notch filter is not necessarily an optimal choice for a DSM's NTF because a notch filter would pass the out of band frequencies about DC, whereas the DSM NTF exhibits no

Reproduced with permission of the copyright owner. Further reproduction prohibited without permission.

particular requirements for the out of band frequencies about DC. As a result, using a notch filter for the NTF of a DSM in a VLIF receiver can lead to a suboptimal design.

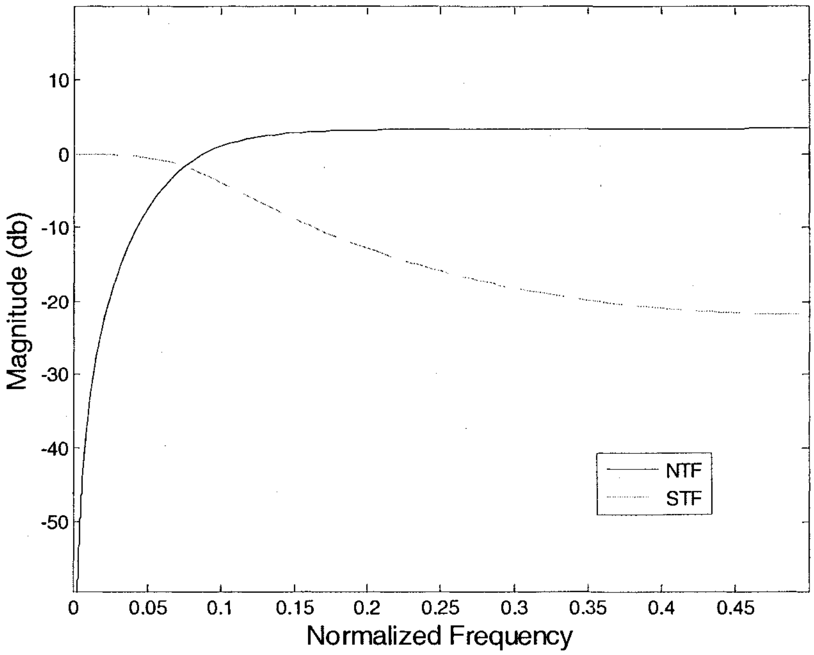

Figure 1: NTF and STF for Typical Second Order DSM

In this thesis, a genetic algorithm is used to generate DSM NTFs that outperform those generated by traditional filter techniques. This algorithm is based on a differential evolution algorithm [1], and unlike previous techniques, this algorithm does not make assumptions about the filter's passband shape or pole-zero placements. The resulting NTFs are compared to baseline designs provided by the delsig toolkit in Matlab [2]. Theses NTFs are then used to design several DSMs which are simulated extensively to compare stability, signal to quantization noise ratio (SQNR), and dynamic range (DR).

Reproduced with permission of the copyright owner. Further reproduction prohibited without permission.

CHAPTER 2

REVIEW OF RELATED LITERATURE

Radio technology has driven innovation since the first demonstration of wireless radio communication in 1893 by Nikola Tesla. The race to develop more reliable communications lead to the tuned radio frequency receiver and then the superhetrodyne receiver, which dominated the radio market until software defined radio architectures were developed in the 1990's [3]. In the later part of the 20th century, digital communications increased in popularity due to their robust error correction, noise suppression, cost, and power efficiency. To reduce the cost of software designed radio, they are often implemented using direct conversion receivers such as ZIF and VLIF receivers. These receivers typically require higher performance ADCs and digital to analog converters (DACs). Delta sigma modulators (DSMs) are a natural choice for digital radio receiver ADCs because of their small size, low power consumption and inherent antialias filtering. Additionally, bandpass DSMs (BPDSMs) are a natural choice for very low intermediate frequency (VLIF) receivers because their NTF's stopband can be tuned about the VLIF.

Traditional techniques for designing DSMs generally use analog filter design techniques, which have been optimized for band select filters but not NTFs. Genetic Algorithms (GA), however, can be optimized to generate NTFs and have been

Reproduced with permission of the copyright owner. Further reproduction prohibited without permission.

successfully used to design IIR filters [4] with constraints such as constant group delay, linear phase, and arbitrary magnitude constraints [5]. Another advantage of GAs is their ability to optimize many parameters at once. Because GAs can optimize many parameters at once, they can often determine solutions that are superior to those determined using traditional approaches. As a result, GAs are well suited for designing DSM NTFs. A specific GA, called Differential Evolution (DE), has been shown to be particularly well suited for filter design [4].

2.1 Tuned Radio Frequency Receiver

In 1916, the Swedish-American Ernst Alexanderson patented the Tuned Radio Frequency Receiver (TRF). Figure 2 shows a block diagram of the basic TRF architecture. In this architecture, the circuits for the radio frequency (RF) amplifier and Tuned Filter stages are separately and manually tuned to the frequency of interest. Manually tuning each stage separately has several difficulties, such as oscillations between the tuned circuits.

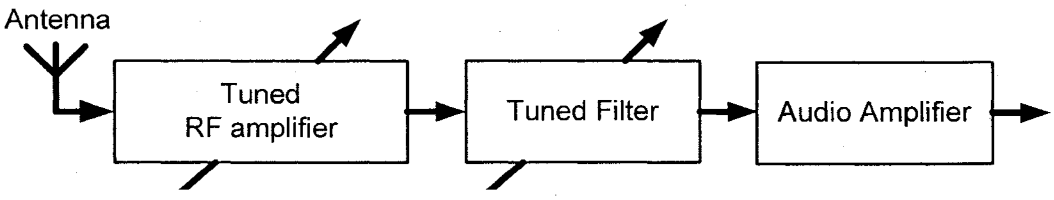

Figure 2: Tuned Radio Receiver Architecture

Reproduced with permission of the copyright owner. Further reproduction prohibited without permission.

2.1.2 Super Heterodyne Receiver

The Super Heterodyne (superhet) receiver resolves many of the problems associated with the TRF architecture. Figure 3 shows a simple block diagram of a typical superhet receiver. As shown in Figure 3, the signal from the antenna is amplified by a tuned RF amplifier. Much like the TRF architecture, the RF amplifier selects a desired frequency, ω_c, using a manually tuned circuit. The resulting signal is mixed with a local oscillator (LO), which is tuned simultaneously with the RF amplifier to the frequency $\omega_c + \omega_{IF}$, where ω_{IF} is the Intermediate Frequency (IF). Because a superhet receiver tunes the RF amplifier and LO together, superhet receivers generate a fixed IF. As a result, a fixed filter, fixed tuned amplifier and fixed demodulator can be used to demodulate the signal. For example, in a typical Amplitude Modulation (AM) receiver, the IF is usually chosen to be 455 kHz. Therefore, for a tuned frequency, ω_c, of 800 kHz the LO would be tuned to ω_c + 455kHz, or 1255 kHz. This LO signal is mixed with the output of the RF amplifier to produce a signal with a carrier frequency of 455 kHz. This IF signal is filtered by a fixed filter and then amplified with a fixed IF amplifier. The resulting signal is then demodulated and sent to an audio amplifier. Because the LO and RF amplifiers are tuned together and because the IF is fixed, the superhet receiver is a much simpler and robust architecture than the TRF receiver.

Reproduced with permission of the copyright owner. Further reproduction prohibited without permission.

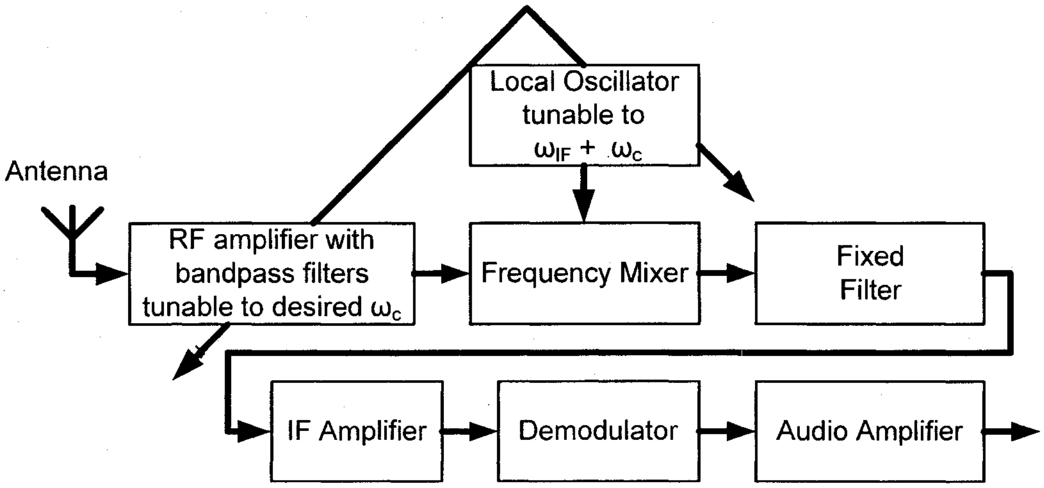
Antenna
Local Oscillator tunable to $\omega_{IF} + \omega_c$
RF amplifier with bandpass filters tunable to desired ω_c
Frequency Mixer
Fixed Filter
IF Amplifier
Demodulator
Audio Amplifier

Figure 3: Typical Super Heterodyne Receiver

2.1.3 Zero Intermediate Frequency (ZIF) and Very Low Intermediate Frequency (VLIF)

Unlike a superhet receiver that mixes the RF signal to an IF before mixing it to DC and demodulating it, a zero IF (ZIF) receiver directly mixes the RF signal to DC. A ZIF receiver is so called because its IF is at DC (or zero frequency). Because the IF is at DC, the demodulator circuitry operates at lower frequencies than superhet demodulators. While ZIF demodulators are often cheaper and consume less power than their superhet counterparts, ZIF circuits are adversely affected by distortion effects and low-frequency noise, such as flicker noise.

Unlike ZIF receivers that mix their IF signals directly to DC, very low IF (VLIF) receiver architectures mix the received signal to a low IF just above the flicker noise. Circumventing this low frequency noise effect can increase the overall signal to noise ratio of the system compared to a ZIF receiver. The use of a VLIF introduces a greater

Reproduced with permission of the copyright owner. Further reproduction prohibited without permission.

level of design complexity to the receiver, but because the VLIF is still very close to DC, VLIF demodulators operate at frequencies similar to ZIF architectures and have costs and power consumption similar to ZIF demodulators.

2.1.4 Complex IF Receivers and Quadrature Signals

Complex IF Receivers use a quadrature mixer to create a quadrature signal which consists of a real, or in phase (I), signal and an imaginary, or quadrature (Q), signal. Quadrature signals are used in many applications, including digital communication systems, radar systems, and antenna beamforming [6]. A system that uses quadrature signals can operate at half the sampling rate that would be required for a system that uses just real signals. Additionally, in systems that use quadrature signals, the information about the phase of the signal is maintained and easily accessible.

Figure 4 shows a block diagram of a quadrature system. The I and Q signals are generated by mixing the RF signal low noise amplifier (LNA) with the complex signal $e^{j2\pi f_c t}$ (or equivalently the signals $\sin(2\pi f_c t)$ and $\cos(2\pi f_c t)$) [6]. For example, if $x(t)$ is mixed with $e^{j2\pi f_c t}$, then

$$x(t)e^{j2\pi f_c t} = x(t)\cos(2\pi f_c t) + j \cdot x(t)\sin(2\pi f_c t)$$

where $x(t)\cos(2\pi f_c t)$ is the real, or in phase, signal and $x(t)\sin(2\pi f_c t)$ is the imaginary, or quadrature, signal. The signals processed by the quadrature mixers are then passed through an anti-aliasing lowpass filter and then converted into digital I and Q signals. The signals can be then be demodulated digitally [6].

In superhet architectures, the channel filters act as anti-aliasing filters. In the VLIF architectures, the LPFs after the mixers act as anti-aliasing filters. As a result, high order filters are required which can be expensive and difficult to fabricate.

Reproduced with permission of the copyright owner. Further reproduction prohibited without permission.

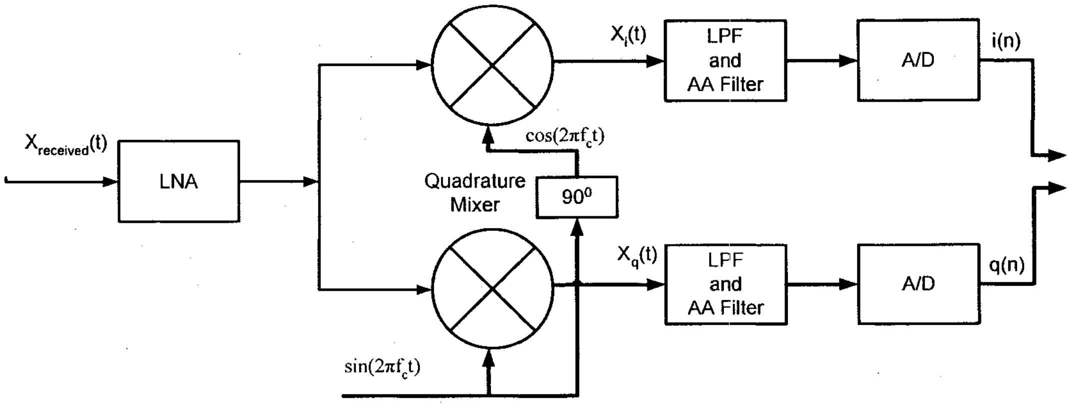

Figure 4: Typical block diagram of a quadrature system

2.2 Analog to Digital Converters

As previously stated, modern receivers have multiple design requirements that are met by converting the signal to digital as soon as possible. Digital signal processing has the advantage of being programmable, cheap, and more quickly designed than comparable analog systems. However, in many receiver systems, the ADC is a significant source of noise [7]. Thus, improving the signal to noise ratio (SNR) of the receiver's ADCs can improve the receiver's SNR. Many different ADC architectures are available.

2.2.1 Parallel ADCs

A Parallel (or flash) ADC converts an analog signal to a digital signal by comparing the analog signal to a set of references. For example, in an 8-bit architecture, $2^8 - 1$ comparators compare the incoming analog voltage signal with $2^8 - 1$ reference voltages which are generated using a resistor string. For example, Figure 5 shows a 3 bit flash converter that has been designed to convert the analog voltages ranging from 0 to 8 volts. The resistor string in Figure 5 sets the reference voltages 1 volt apart. When the

Reproduced with permission of the copyright owner. Further reproduction prohibited without permission.

analog input voltage v_i is less than 0.5 volts, all the comparators are low. As the voltage increases, more comparators switch high. The encoding logic encodes the digital outputs from the comparators into an appropriate digital code. The flash ADC is classified as a *Nyquist converter* because it can sample analog signals at their Nyquist frequency. In practice, flash converters usually sample at a rate slightly higher than the Nyquist rate. Flash converters are also used as building blocks for other architectures.

Although the flash converter uses a fast and simple method to digitize analog signals, their performance is limited by the precision of the components used to make them. For example, resistor mismatch is a continuing problem in current CMOS processes. Also, comparators in this architecture must be able to accurately switch on voltages within half of the least significant bit (LSB). Process variations in doping density, resistance, capacitance, and carrier mobility limit the accuracy of comparators. Currently, CMOS technology limits this precision to about 0.02% [7].

To illustrate how this limits a flash converter, consider an N-bit flash converter that has 2^N comparators. Each comparator's threshold is separated by (*dynamic range*) * 2^{-N} volts. Because CMOS processes limit a comparator's precision to 0.02%, the voltage between each voltage reference cannot change by more than 0.02%. 2^N resistors will produce 2^{-N} voltage reference increments. Setting $2^{-N} = 0.0002$ implies that $N \approx 12$, which is largest number of bits that can be used before the reference voltages generated will be less than 0.02%. This upper limit is referred to as the effective number of bits (ENOB); that is, the digital circuitry will not be capable of resolving more than a 12 bit flash converter.

Reproduced with permission of the copyright owner. Further reproduction prohibited without permission.

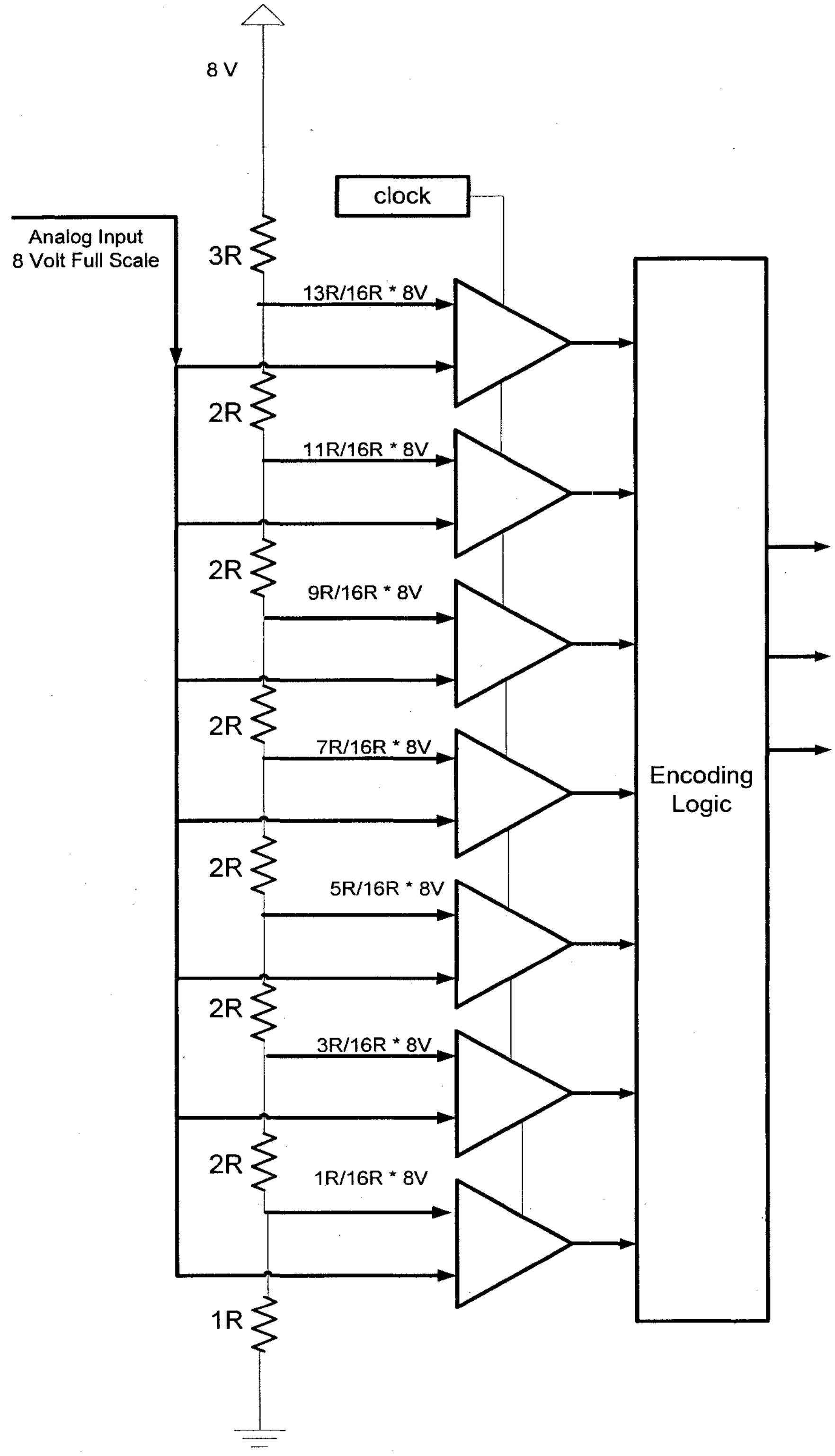

Figure 5: Block Diagram of a Simple Flash Decoder

Reproduced with permission of the copyright owner. Further reproduction prohibited without permission.

Even though CMOS processes are becoming more accurate, other concerns make the flash converter problematic for use in modern systems. An *N*-bit converter requires 2^N comparators and 2^N resistors. As a result, the size and power consumption of the flash ADC grows exponentially with the number of bits. This exponential growth limits their use to applications that require 8 bits or less.

2.2.2 Delta Sigma Modulator

The delta sigma modulator (DSM) is an ADC which can attain a high ENOB by using a flash converter with a smaller number of bits, but at the cost of increased sampling frequency [8]. Implementations in the continuous-time domain are referred to as continuous time DSMs and use integrators. Implementations in the discrete-time domain are often referred to as discrete-time DSMs and use an accumulator instead of an integrator. Figure 6 shows a first order continuous-time DSM and Figure 7 shows a first order discrete-time DSM. The difference (the delta) of the DSM's input and DSM's output feedback through the DAC is integrated, or accumulated, (the sigma) and fed through an ADC. Often a DSM's ADC is a one bit converter which can be implemented using a clocked comparator. A DSM is classified as an *oversampled converter* because it samples at a frequency that is much higher than the Nyquist rate. The oversampling ratio (OSR) is the ratio of a DSM's sampling frequency to the signal's Nyquist frequency. The OSR for a DSM is typically between 8 and 1024.

Reproduced with permission of the copyright owner. Further reproduction prohibited without permission.

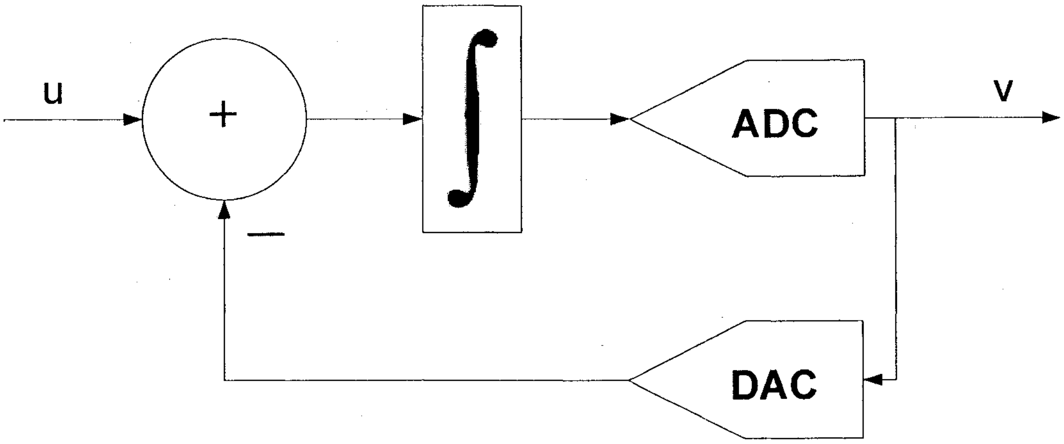

Figure 6: Continuous Time DSM

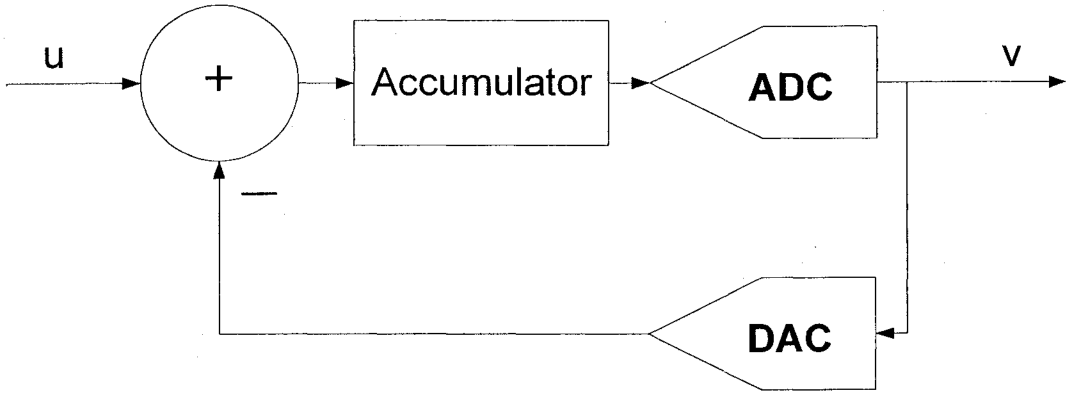

Figure 7: A Discrete-Time DSM

Because ADCs are nonlinear components, DSMs are nonlinear systems. Furthermore, the memory elements inherent in ADCs cause DSMs to be dynamic, time varying systems. These properties make mathematical analysis of DSMs difficult. Analysis of DSMs in the time domain is a useful exercise to help understand the basic

Reproduced with permission of the copyright owner. Further reproduction prohibited without permission.

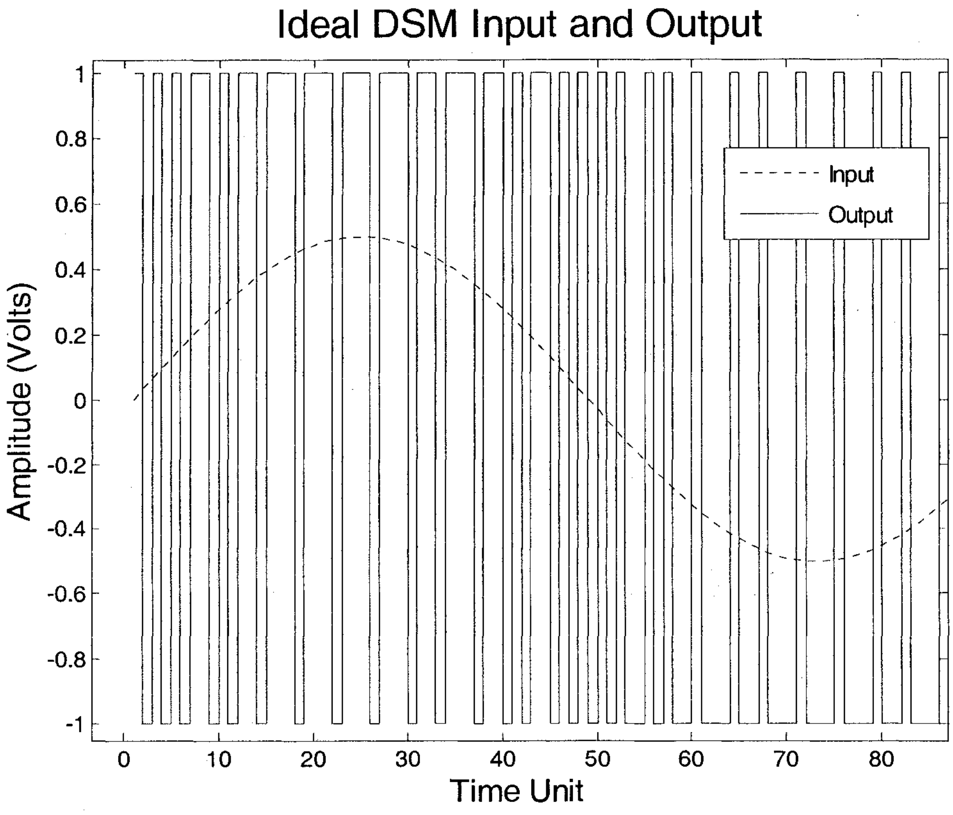

Figure 8: Ideal DSM input and Output

mechanics of a DSM, but more insight can often be gained by using a linearized model and examining the DSM's STF and NTF.

2.2.1 Time Domain Analysis of the DSM

To illustrate some of the properties of the DSM, consider the bitstream produced by the first order DSM shown in Figure 7 where the DSM's input is the sine wave shown in Figure 8. The first few samples of the sine wave are 0.033, 0.067, and 0.1. Assuming the output of the DAC is initialized to -1, the first accumulator output is simply 1.033. Because 1.033> 0, the ADC output (which is the DSM's output) is 1, which is fedback and subtracted from the next input sample 0.067. Now, the input to the accumulator is 0.067 -1, or -0.933. This is added to the previous accumulator value of 1.033. This yields

Reproduced with permission of the copyright owner. Further reproduction prohibited without permission.

0.0100 which causes the ADC output to be 1. Continuing these steps, the results in Table 1 are obtained.

In general, the average of the comparator's output tracks the average of the input signal [8]. This shows a correlation between the modulator output and input, but a more useful model for analysis is developed in the frequency domain.

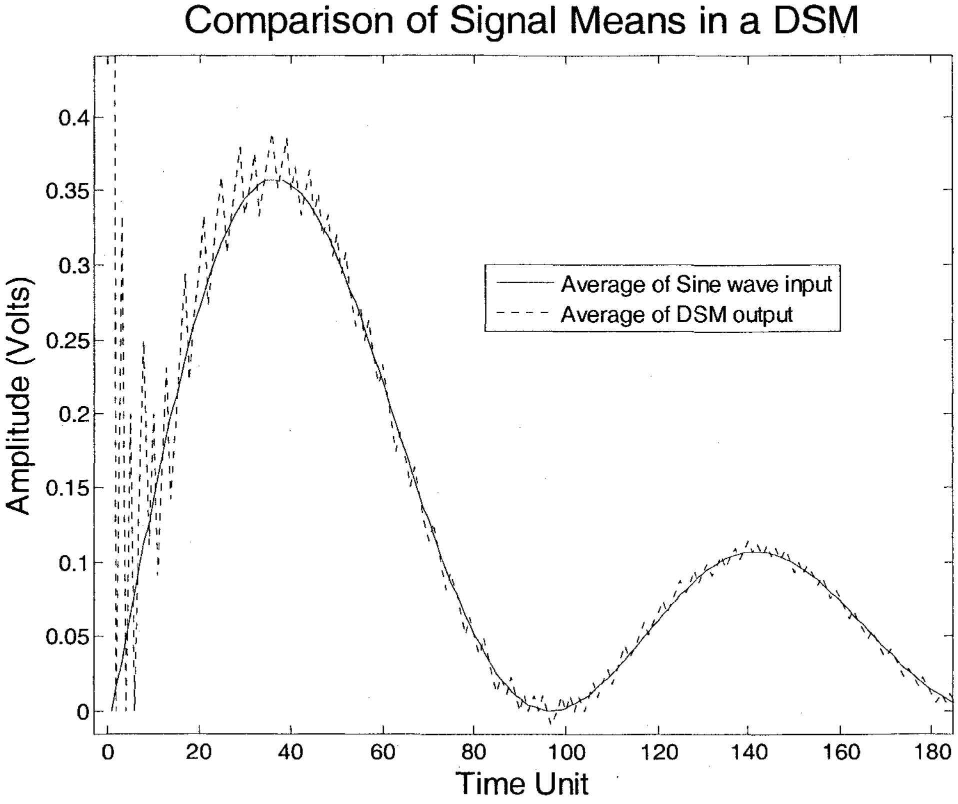

Figure 9: The Mean of the Input and Output signals

Reproduced with permission of the copyright owner. Further reproduction prohibited without permission.

Iteration	**Input**	**Diff.**	**Acc.**	**Out**	**Input Average**	**Output Average**	**Error**
0	0	0	0	-1	0	-1	-
1	0.033	1.033	1.033	1	0.017	0.000	100.0%
2	0.067	-0.933	0.100	1	0.033	0.333	-900.6%
3	0.100	-0.900	-0.800	-1	0.050	0.000	100.0%
4	0.133	1.133	0.333	1	0.067	0.200	-200.6%
5	0.166	-0.834	-0.501	-1	0.083	0.000	100.0%
6	0.199	1.199	0.697	1	0.100	0.143	-43.4%
7	0.231	-0.769	-0.071	-1	0.116	0.000	100.0%
..	...	...	...	...	...	...	...
143	-0.999	0.001	-1.129	-1	0.194	0.194	-0.5%
144	-0.996	0.004	-1.126	-1	0.185	0.186	-0.5%
145	-0.993	0.007	-1.118	-1	0.177	0.178	-0.5%
146	-0.988	0.012	-1.106	-1	0.169	0.170	-0.4%
147	-0.982	0.018	-1.089	-1	0.162	0.162	-0.4%
148	-0.976	0.024	-1.065	-1	0.154	0.154	-0.3%

Table 1: Values of a 1 bit DSM in operation

2.2.2.2 Linear Model of DSM

Because of the complexity associated with the analysis of the nonlinear quantizer, DSMs are often analyzed using a linearized model. Figure 10 shows an example of a 1st order discrete time DSM where z^{-1} represents a delay. In this linear model, the quantizer is modeled as an additive noise source. To analyze this DSM note that

$$V(z) = Y(z) + E(z) \tag{2.1}$$

and

$$Y(z) = z^{-1}Y(z) + U(z) - z^{-1}V(z). \tag{2.2}$$

Reproduced with permission of the copyright owner. Further reproduction prohibited without permission.

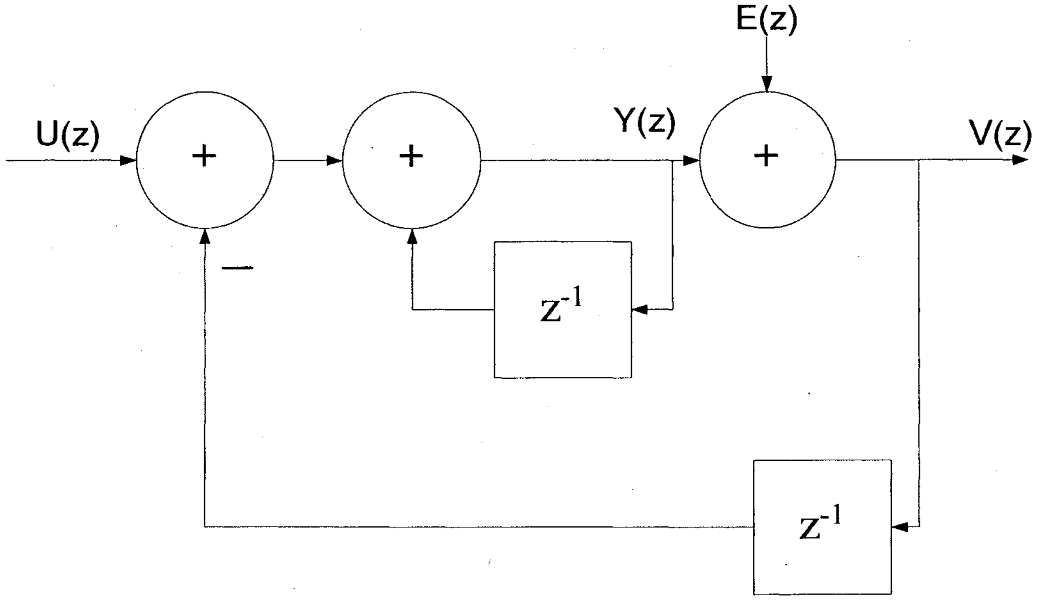

Figure 10: Linearized First Order DSM Model

Substituting (2.2) into (2.1) yields

$$\begin{aligned} V(z) &= z^{-1}Y(z) + U(z) - z^{-1}V(z) + E(z) \\ &= U(z) + E(z) - z^{-1}(V(z) - Y(z)) \\ &= U(z) + E(z) - z^{-1}E(z) \\ &= U(z) + (1 - z^{-1})E(z) \qquad (2.3) \end{aligned}$$

Because the DSM's STF is the transfer function from the DSM's input to the DSM's output and because the DSM's NTF is the transfer function from the DSM's additive noise source to the DSM's output, (2.3) can be written as

$$V(z) = STF(z) \cdot U(z) + NTF(z) \cdot E(z)$$

where

$$STF(z) = 1$$

and

$$NTF(z) = (1 - z^{-1}).$$

Reproduced with permission of the copyright owner. Further reproduction prohibited without permission.

Because *STF(z)* = 1, all input signals are passed unfiltered. Figure 11 shows the frequency response of *NTF*(*z*). This plot shows that the quantization noise is suppressed at frequencies near DC.

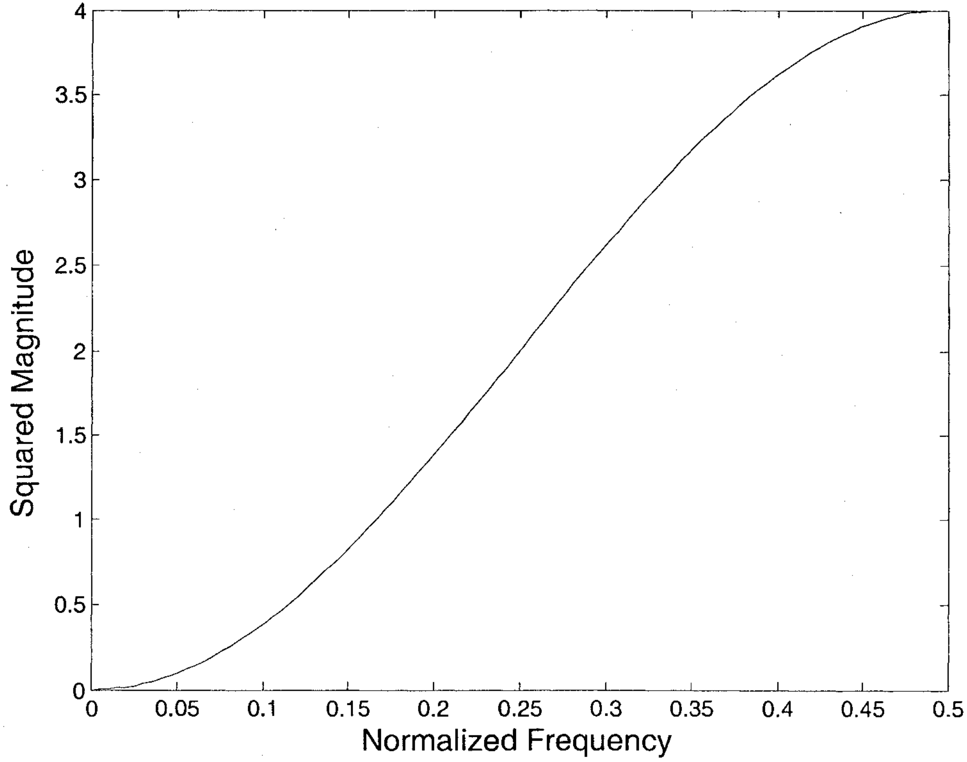

Figure 11: Squared Magnitude Response for NTF Predicted by Linear Model

Increasing the performance of a DSM can be accomplished in a number of different ways. One method is to choose a band of interest closer to DC. As discussed earlier, this may allow the signal to operate in a region where the NTF is lower; however, in many applications the band of interest cannot be chosen lower. Another method is to increase the OSR. This has the same effect as lowering the band of interest frequency; however, increasing the OSR requires faster (and more expensive) circuitry. Another

Reproduced with permission of the copyright owner. Further reproduction prohibited without permission.

method is to shape the NTF so that its magnitude response is lower within the signal band. This requires a higher order DSM.

2.2.2.3 Higher Order DSM

Although increasing a 1st order DSM's OSR can improve its performance, a first order DSM is not always a feasible design choice. For example, some applications may require such a high OSR that the required sampling rate of the quantizer is above technological (or economical) limits. In such cases, a higher order DSM can be used. Figure 12 shows a linearized model of a second order DSM where the ADC has been modeled as an additive noise source. To determine the 2nd order DSM's output, note that by inspection of Figure 12

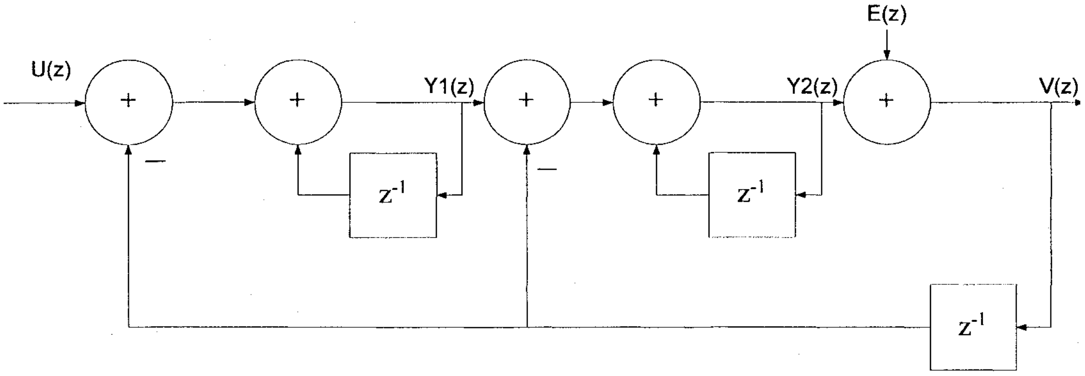

Figure 12: Second Order Discrete Time Delta-Sigma Modulator

$$V(z) = Y_2(z) + E(z) \tag{2.4}$$

$$Y_2(z) = z^{-1}Y_2(z) + Y_1(z) - z^{-1}V(z) \tag{2.5}$$

and

$$Y_1(z) = z^{-1}Y_1(z) + U(z) - z^{-1}V(z)\,. \tag{2.6}$$

Solving (2.6) for $Y_1(z)$ and (2.5) for $Y_2(z)$ yields

Reproduced with permission of the copyright owner. Further reproduction prohibited without permission.

$$Y_1(z) = \frac{U(z) - z^{-1}V(z)}{1 - z^{-1}} \tag{2.7}$$

and

$$Y_2(z) = \frac{Y_1(z) - z^{-1}V(z)}{1 - z^{-1}}. \tag{2.8}$$

Substituting (2.7) into (2.8) yields

$$\begin{aligned} Y_2(z) &= \frac{U(z) - z^{-1}V(z)}{(1 - z^{-1})^2} - \frac{z^{-1}V(z)}{1 - z^{-1}} \\ &= \frac{U(z)}{(1 - z^{-1})^2} - \frac{(2z^{-1} - z^{-2})V(z)}{(1 - z^{-1})^2}. \end{aligned} \tag{2.9}$$

Substituting (2.9) into (2.4) yields

$$V(z) = \frac{U(z)}{(1 - z^{-1})^2} - \frac{(2z^{-1} - z^{-2})V(z)}{(1 - z^{-1})^2} + E(z)\ .$$

Therefore,

$$V(z)\frac{(1 - z^{-1})^2 + 2z^{-1} - z^{-2}}{(1 - z^{-1})^2} = \frac{U(z)}{(1 - z^{-1})^2} + E(z)$$

which implies that

$$V(z)\frac{1}{(1 - z^{-1})^2} = \frac{U(z)}{(1 - z^{-1})^2} + E(z). \tag{2.10}$$

Substituting (2.10) for $V(z)$,

$$V(z) = U(z) + (1 - z^{-1})^2 E(z).$$

Therefore, the output of the 2nd order DSM can be written as

$$V(z) = STF(z)U(z) + NTF(z)E(z)$$

Reproduced with permission of the copyright owner. Further reproduction prohibited without permission.

where

$$NTF(z) = (1-z^{-1})^2$$

and

$$STF(z) = 1.$$

Figure 13 shows a plot of the magnitude response for both the first and second order DSMs' NTFs. Note that the second order DSM's NTF provides a lower response close to DC, but this is traded for higher overall noise in the NTF.

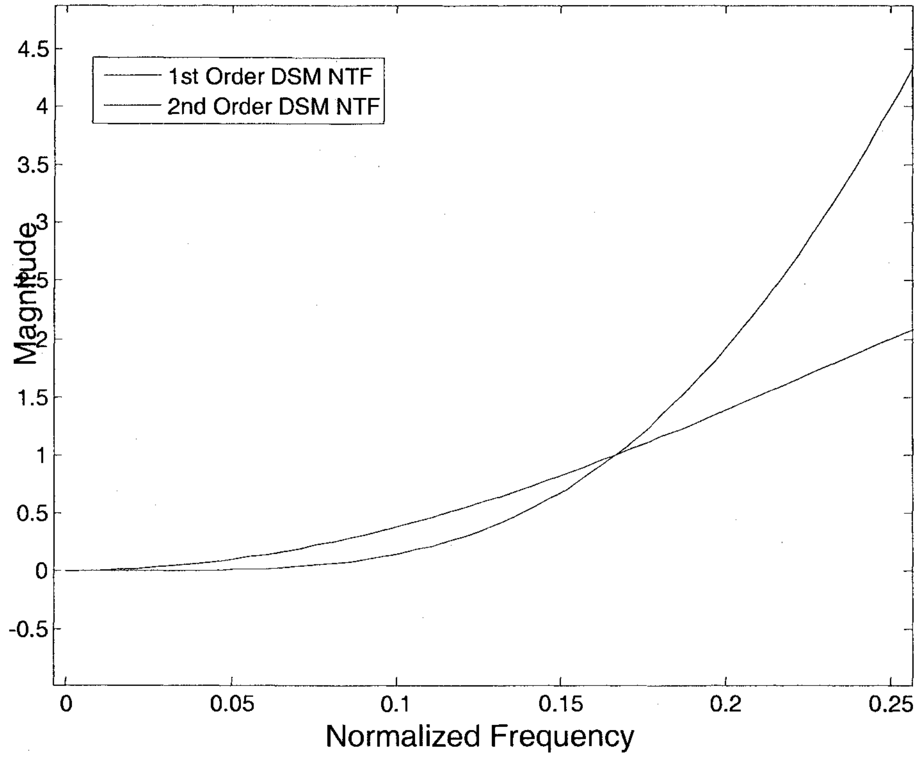

Figure 13: Squared Magnitude Response for 1st and 2nd Order DSM NTFs

Reproduced with permission of the copyright owner. Further reproduction prohibited without permission.

2.2.2.4 Realizability

Because discrete systems cannot be implemented with delay free loops, the feedback loop of a DSM must contain at least one delay. As a result, a DT DSM's impulse response, $h(n)$, at the time zero is one; that is, $h(0) = 1$. To illustrate, consider the DSM shown in Figure 10. The output from Figure 10, $v(n)$, can be written as

$$v(n) = y(n) + e(n).$$

Assuming that $y(-1) = 0$ and $e(-1) = 1$,

$$v(-1) = y(-1) + e(-1) = 0 + 1 = 1$$

Therefore, if $u(n) = \delta(n)$

$$v(0) = y(0) + y(-1) + e(0) = 0 + 0 + 1 = 1, \tag{2.11}$$

and thus $h(0) = 1$. Therefore,

$$\lim_{z \to \infty} H(z) = \lim_{z \to \infty} \sum z^{-n} h(n) = h(0) = 1$$

This constraint due to the feedback loop delay limits a designer's flexibility when designing NTFs.

2.2.2.5 Zero Optimization

In [2], a design technique is described that generates DSM NTFs that attenuate the quantization noise across the band of interest. This technique determines optimal NTF zeroes by minimizing the quantization noise power over the band of interest. In particular, the technique sets the first derivative of the in-band power spectral density (PSD) to zero and solves for the optimal zeroes. After determining the optimal zeroes, the NTF's poles are optimized using an iterative approach. The results of this procedure for a DSM with an OSR of 32 are reprinted in Table 2. All the zero locations have been

Reproduced with permission of the copyright owner. Further reproduction prohibited without permission.

normalized so that OSR multiplied by the passband bandwidth, ω_B, is 1. ω_B is expressed in radians / sample.

N	Zero Locations, Normalized to ω_B	SQNR Improvement
1	0	0
2	$\pm 1/(\sqrt{3})$	3.5 dB
3	$0,\pm\sqrt{3/5})$	8 dB
4	$\pm(\sqrt{3/7 \pm \sqrt{(3/7)^2 - 3/35}})$	13 dB
5	$0,\pm(\sqrt{5/9 \pm \sqrt{(5/9)^2 - 5/21}})$	18 dB
6	$\pm 0.23862,\pm 0.66121,\pm 0.93247$	23 dB
7	$0,\pm 0.40585,\pm 0.74153,\pm 094911$	28 dB
8	$\pm 0.18343,\pm 0.52553,\pm 0.79667,\pm 0.96029$	34 dB

Table 2: Optimized Zeros Found by Schreier for an OSR of 32

2.2.2.6 Pole Optimization

Higher order DSMs are often difficult to stabilize. Additional feedback loops are often used to stabilize higher order DSMs. For example, consider the first order DSM in Figure 7. The added feedback loop introduces another pole into the system which is often used to give the system greater stability and a better NTF at low frequencies. By inspection of the block diagram in Figure 10,

$$Y(z) = z^{-1}Y(z) + U(z) - a_1 z^{-1} V(z) \qquad (2.12)$$

and

Reproduced with permission of the copyright owner. Further reproduction prohibited without permission.

$$V(z) = Y(z) + E(z) - a_2 z^{-1} V(z). \tag{2.13}$$

(2.12) implies that

$$Y(z) = \frac{U(z) - a_1 z^{-1} V(z)}{1 - z^{-1}}, \tag{2.14}$$

and (2.13) implies that

$$V(z) = \frac{Y(z) + E(z)}{1 + a_2 z^{-1}} \quad . \tag{2.15}$$

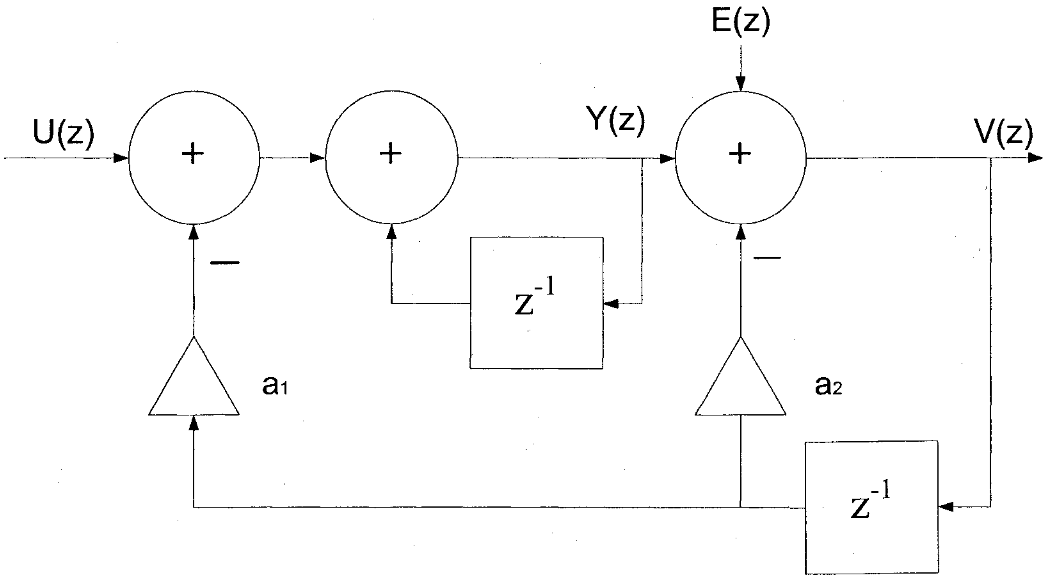

Figure 14: Generalized First Order DSM Topology

Substituting (2.14) into (2.15) yields

$$V(z) = \frac{U(z) - a_1 z^{-1} V(z)}{(1 - z^{-1})(1 + a_2 z^{-1})} + \frac{E(z)}{1 + a_2 z^{-1}} \ . \tag{2.16}$$

Solving (2.16) for *V(z)* yields

Reproduced with permission of the copyright owner. Further reproduction prohibited without permission.

$$V(z)\frac{(1-z^{-1})(1+a_2z^{-1})+a_1z^{-1}}{(1-z^{-1})(1+a_2z^{-1})}=\frac{U(z)}{(1-z^{-1})(1+a_2z^{-1})}+\frac{E(z)}{1+a_2z^{-1}}$$

$$V(z)\frac{1+(-1+a_1+a_2)z^{-1}-a_2z^{-2}}{(1-z^{-1})}=\frac{U(z)}{(1-z^{-1})}+E(z)$$

$$V(z)=\frac{U(z)+E(z)(1-z^{-1})}{1+(-1+a_1+a_2)z^{-1}-a_2z^{-2}},$$

or equivalently,

$$V(z)=STF(z)U(z)+NTF(z)E(z)$$

where

$$STF(z)=\frac{1}{1+(-1+a_1+a_2)z^{-1}-a_2z^{-2}}$$

and

$$NTF(z)=\frac{(1-z^{-1})}{1+(-1+a_1+a_2)z^{-1}-a_2z^{-2}}. \qquad (2.17)$$

Notice that the a_2 term in (2.17) increases the order of the NTF but not the number of inband zeros. In many applications, the a_2 feedback is not needed and in such cases is set to zero. Assuming a_2 is zero, (2.17) can be written as

$$NTF(z)=\frac{(1-z^{-1})}{1+(-1+a_1)z^{-1}} \qquad (2.18)$$

Reproduced with permission of the copyright owner. Further reproduction prohibited without permission.

The NTF in (2.18) has its zero at $z = 1$ and its pole at $z = (1 - a_1)$. The NTF can then be optimized by selecting a gain a_1 such that the in-band noise is minimized. The NTF gain determines its stability and realizability [9].

As discussed in section 2.2.2.4, a DSM must have NTF(∞) = 1. Also, some rules of thumb exist that limit the maximum NTF gain to be < 1.5 for the DSM to be stable [10].

2.2.3 Bandpass DSM

For VLIF receivers, a bandpass DSM can outperform a lowpass DSM because the NTF is designed to minimize the SQNR around the VLIF. Bandpass DSMs (BPDSM) are often used in narrowband applications where they can achieve a high SQNR with a relatively low OSR and DSM order. Figure 15 shows an example of a NTF and STF for a BPDSM.

Bandpass DSM (BPDSM) NTFs are often designed by transforming a lowpass DSM using transformations such as the n-path or Z transforms. Transformation techniques are advantageous because the resulting BPDSM NTF has many of the same properties as its lowpass equivalent, and little work needs to be done to analyze the new NTF.

Reproduced with permission of the copyright owner. Further reproduction prohibited without permission.

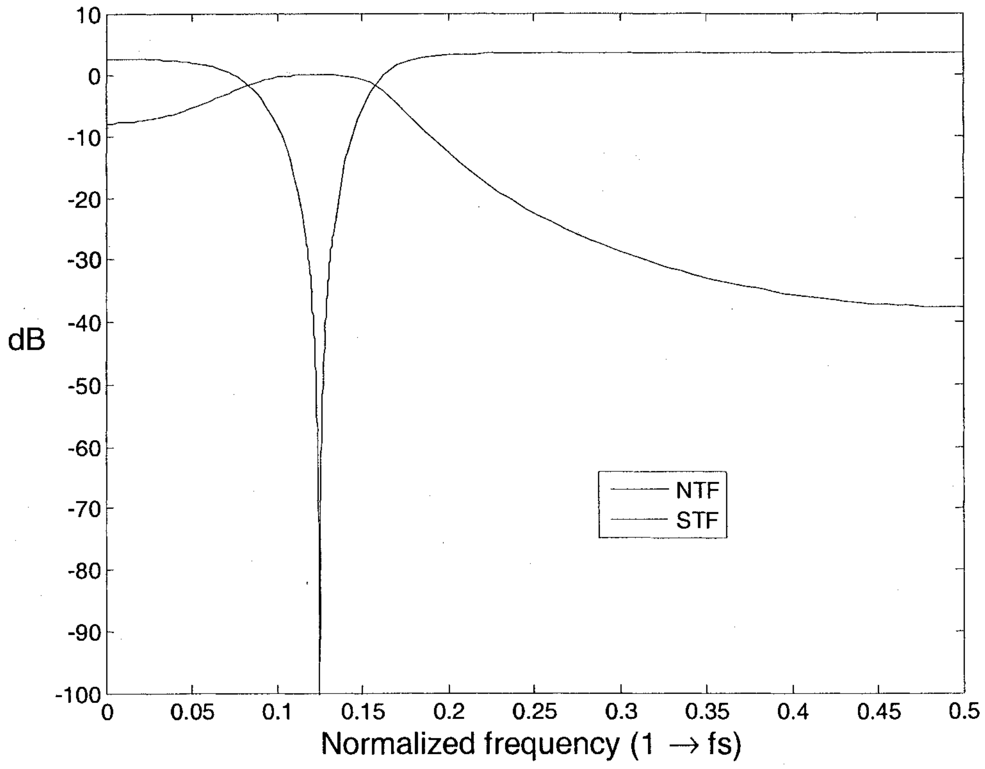

Figure 15: Typical Magnitude response for a BPDSM with $f_0 = 0.125$

2.2.4 DSM Design

The first step in designing a DSM is to determine a STF and NTF that can meet the desired requirements. The STF is typically designed to have a constant gain over the frequency band of interest. The NTF is designed to suppress noise as much as possible in the frequency band of interest. After determining the STF and NTF, an implementation topology is chosen. The literature describes several different topologies, each of which has distinct advantages and disadvantages [5] [11] [12] [13] [14] [15].

2.2.4.1 Stability

Reproduced with permission of the copyright owner. Further reproduction prohibited without permission.

Because a DSM's quantizer always generates a bounded output of ±1, a DSM is always stable in the classic Bounded-Input Bounded-Output (BIBO) stability sense. Nevertheless, even though the output is bounded, the DSM can enter a limit cycle which causes the DSM's SNR to decrease significantly. The stability of a DSM is thus a viewed as the ability for the DSM to follow the predictions provided by the linear model.

Several methods such as root locus, Nyquist, and statistical gain modeling can be used to predict the stability of a DSM; however, these methods are only valid for linear systems, and therefore extensive simulations are needed to verify a DSM's stability.

2.3 Adaptive Algorithms

An adaptive algorithm is an algorithm that changes a system to perform according to some well defined criterion [16]. Adaptive algorithms have been used in many applications including modeling, estimation, optimization, and prediction. Many adaptive algorithms use an objective function (also called a cost function) to adjust parameters. For some such algorithms, conditions such as convergence, time out or stall are used to stop an algorithm. Convergence occurs if the objective function value is lower than some predetermined value. An algorithm is timed out if the iteration is greater than some specified value. Also, the algorithm may be stopped if no better value has been found for some number of iterations. This is termed a stall conditioned.

2.3.1 Learning Curves and Convergence

Many adaptive algorithms change the weights (coefficients) of the terms in a polynomial or difference equation. As the coefficients change and the adaptive system converges, the objective function produces a smaller cost which implies that the system is

Reproduced with permission of the copyright owner. Further reproduction prohibited without permission.

converging to a solution. An adaptive algorithm's learning curve is defined as the objective function value as a function of iteration number. Figure 16 shows an example of a learning curve. The curve flattens out as the system converges to a stable value. The rate at which the learning curve converges is one figure of merit used when comparing adaptive algorithms.

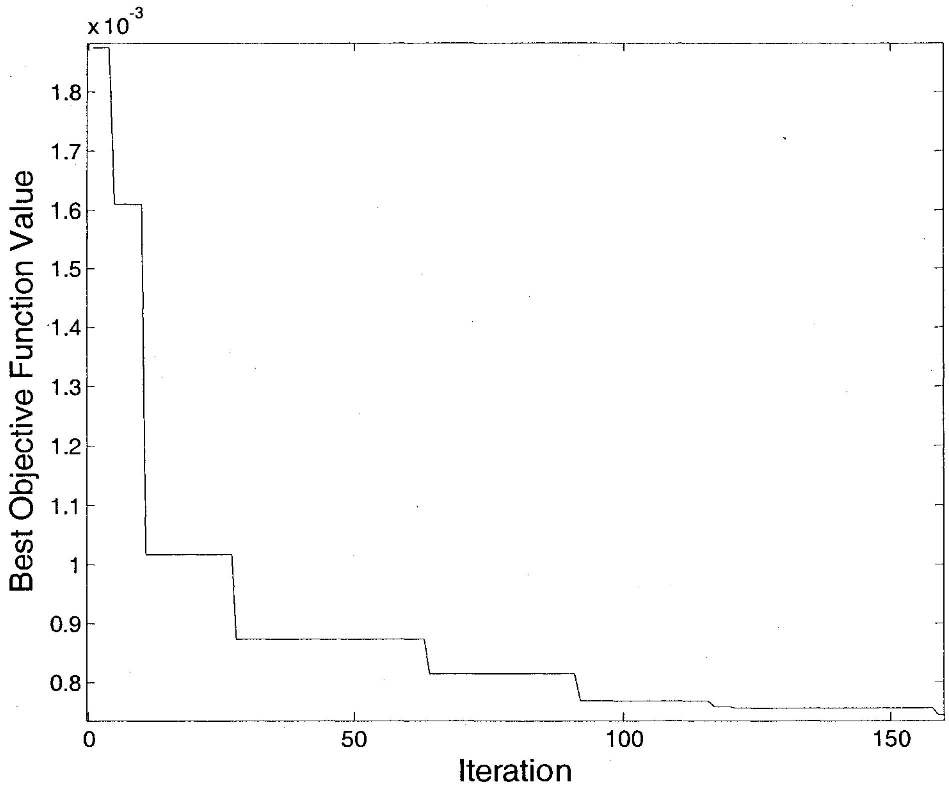

Figure 16: Typical Learning Curve for an Adaptive Algorithm

2.3.2 Errors in Convergence

Adaptive algorithms tradeoff convergence speed for accuracy. When an adaptive algorithm changes the weights of the system by a large amount each iteration, the algorithm converges quickly. However when the weights change by a large amount each

Reproduced with permission of the copyright owner. Further reproduction prohibited without permission.

iteration, the system can "bounce around" an optimal answer. Also, if too large a factor is chosen, the algorithm may become unstable and diverge. On the other hand, an algorithm that changes its weights by a smaller amount converges more slowly but can converge closer to an optimal answer. Changing the weights by small amounts, however, can cause the system to take much longer to converge and waste computation time.

Errors can also be caused by polymodal cost functions. An adaptive algorithm with a polymodal cost function can converge to a local and not global minimum. A robust algorithm is needed that can disregard local minima and correctly find the global minimum. Several tests [1] have been developed to test the robustness of an adaptive algorithm's ability to find global minima.

2.3.3 LMS Adaptation and the Equation Error Method

The least-mean-square (LMS) algorithm is an adaptive algorithm that can be used to design filters by use of the Equation Error Method [17]. This method was initially considered for the design of BPDSM in this thesis and converged to an optimal solution for low order DSMs; however it was unable to converge for higher order DSMs.

2.3.4 Genetic Algorithms

Genetic algorithms (GA) are adaptive algorithms that search a cost function for its optimal solution by using a biological paradigm [18]. For GAs, a vector of weights is called a population vector, and all the population vectors form the population. For DSM design, elements of a population vector could be the coefficients of the NTF's difference equation or the phases and magnitudes of the NTF's poles and zeros.

A GA compares various population vectors with one another to determine the fittest population vectors within the population. The fittest population vectors are those

Reproduced with permission of the copyright owner. Further reproduction prohibited without permission.

that generate the lowest costs. After determining a group of the fittest population vectors, these fittest vectors are combined in various ways to create new vectors that are once again compared for fitness. Each iteration of generating and comparing population vectors is referred to as a new generation. Different types of genetic algorithms differ in how many vectors are carried on to the next generation, how new vectors are created and how old vectors are treated. However, regardless of the type of GA, all GAs allow the fittest vectors with the lowest cost to replicate and form the next generation by some method. Other common GA characteristics include the fittest members of a population to share some of their elements with other members of the population (recombination/crossover), adding random variations to ensure that genetic diversity (mutation) is maintained, and allowing two fit individuals to combine into an entirely new vector which is a combination of the two (sexual reproduction).

2.3.4.1 Differential Evolution

Differential Evolution (DE) is a GA that was developed by Dr. Rainer Storn [1]. Consider a system where all the properties of the system are dependent on real constants. The vector **P** is the population vector, where

$$\mathbf{P}=[p_1, p_2, p_3, \ldots, p_D]^T, \tag{2.19}$$

p_1, p_2, p_3 … p_D are real numbers and D is the number of independent parameters. The parameters are then are evaluated based on a set of objectives and constraints. An objective is a functional metric that maps the vector, **P**, to a real value such as SNR, the in band rms noise, or a weighted sum of the two. Constraints are one or more equalities or inequalities that the solution must satisfy. Constraints such as a maximum out of band gain or forcing all poles to lie within the unit circle confine the solution space.

Reproduced with permission of the copyright owner. Further reproduction prohibited without permission.

Optimizing the system entails developing an objective function $J(x)$ that incorporates all objectives and constraints. This function is then minimized using the DE method described below.

In DE, a given generation, **G**, contains N D x1 population vectors, $\mathbf{P}_k$ for $k=1,\ldots N$; that is,

$$\mathbf{G} = [\mathbf{P}_1 \,|\, \mathbf{P}_2 \,|\, \mathbf{P}_3 \,|\, \ldots \,|\, \mathbf{P}_N]$$

where **G** is an N x D matrix. For the first generation, **G** is initialized with random values that have a uniform distribution unless some information is known about the solution. In such cases, **G** is initialized such that the solution is within its span. A trial vector, $\mathbf{U}_i$ is created by setting $\mathbf{U}_i = \mathbf{P}_i$, where $\mathbf{P}_i$ is the ith population vector in **G**. A variation vector **V** is then created by taking the difference of two distinct population vectors and multiplying their difference by the differential variation factor μ, and adding this product to another distinct population vector. Finally, **U** adopts some of the parameters from **V**, depending on the crossover probability CR. Thus this process can be described by

```
for $i = 1$ to $N$,
    $\mathbf{U}_i = \mathbf{P}_i$
    $\mathbf{V} = \mathbf{P}_x + \mu\,(\mathbf{P}_y - \mathbf{P}_z)$   where $x \neq y \neq z$
    $u_{i,j} = v_{i,j}$   for   $j = \langle n \rangle_D, \langle n+1 \rangle_D, \ldots, \langle n+L-1 \rangle_D$
```

where $\langle\,\rangle_D$ is the modulo function with modulus D, n is a randomly chosen integer between 1 and D with equal probability density, and L is a random integer from 1 to D, with probability $Pr(L=v) = (CR)^v$. Figure 17 shows an example case for $D = 5$, n is 3, and $L = 4$.

Reproduced with permission of the copyright owner. Further reproduction prohibited without permission.

The trial vector $\mathbf{U}_i$ is evaluated and compared to the value of the original vector $\mathbf{P}_i$. The better of the two is kept as the new $\mathbf{P}_i$. This process continues until all population vectors have been evaluated against a constructed trial vector and tested for fitness. The vector with the lowest cost is saved to keep track of the progress of the algorithm. The process continues with a new generation consisting of the winners of the previous generation until an exit condition is satisfied.

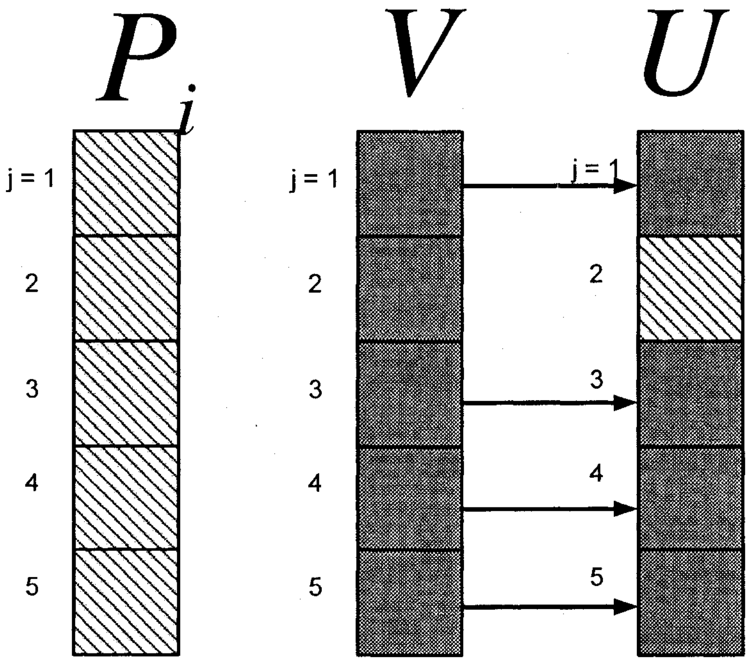

Figure 17: Example of Trial Vector being formed via the Crossover Process

Reproduced with permission of the copyright owner. Further reproduction prohibited without permission.

CHAPTER 3

ADAPTIVE DESIGN METHODOLOGY

In this chapter, a process that uses differential evolution to design delta sigma modulators is described. A comparison is then drawn between this method and a traditional DSM design method using the delsig Matlab toolbox.

3.1 DSM Design using Differential Evolution

It has been shown that GAs such as DE lend themselves to filter design well. Because an NTF is essentially an IIR filter, GA techniques can be applied to DSM design. Additionally, unlike traditional methods of optimizing NTFs which typically assume a specific filter shape, GAs can optimize for complex filter specifications, and as a result they can generate DSMs with a lower SQNR for a given order and OSR. As a result, a genetic algorithm such as Differential Evolution can find NTFs which could not be generated using traditional design techniques.

3.1.1 Population Vector and Cost Function

Checking stability of an NTF is more easily accomplished by using its poles rather than the coefficients of its describing difference equation. Because of this, a population vector consisting of the magnitude and angle for each zero and pole was chosen. Assuming that the DSM is a real, system implies that the poles and zeros are

Reproduced with permission of the copyright owner. Further reproduction prohibited without permission.

either real or appear in complex conjugate pairs. Because of the symmetry of the complex parameters, only half of a conjugate pair needs to be stored and manipulated. Also, since an odd order DSM will have one real pole and one real zero, their angles are always zero and do not need to be stored. Therefore a population vector ***P***, for an NTF with real coefficients can be described by

$$\boldsymbol{P} = [az_1, az_2, \ldots az_i, ap_1, ap_2, \ldots ap_j, mp_1, mp_2, \ldots mp_j],$$

where az_k is the *k*th zero angle, ap_k is the *k*th is a pole angle, mp_k is the *k*th pole magnitude, and i is (order / 2) rounded down and j is (order / 2) rounded up.

To develop a DE cost function for designing optimal DSMs, the cost function must include the NTF's critical design parameters, which are stability, desired signal to quantization ratio (SQNR) over the band of interest and dynamic range over the band of interest. In [2], Schreier suggests that reducing the total quantization noise within the band of interest leads to a higher SQNR, but only so long as the frequency response's out of band infinity norm is less than 1.5. This criterion is know as Lee's rule of thumb, and is often used as a stability criterion in DSMs [9]. Based on the above criterion, the following cost function was developed:

```
if ( $maxpolemag > 1$ )
        $PoleError = maxpolemag*100000;$
else
        $PoleError = 0;$
end if
```

Reproduced with permission of the copyright owner. Further reproduction prohibited without permission.

```
if ($\|H\|_\infty <$ maximum allowable $\|NTF(e^{j\omega})\|_\infty$)
    $J(x_k) = IBG + DR*DRFactor + PoleError$
else
    $J(x_k) = 1000*(100*IBG + DR*DRFactor + \|NTF(e^{j\omega})\|_\infty) + PoleError$
end if
```

where J is the cost function, x_k is the population vector being evaluated, DR is the dynamic range in the band of interest, IBG is the inband gain of the NTF, $DRFactor$ is an optimization factor used to place emphasis on high DR designs, and $\|NTF(e^{j\omega})\|_\infty$ is the infinity norm of the NTF's frequency response. The term *maxpolemag* is the largest pole magnitude. It is weighted heavily when its value is greater than one to ensure that an unstable pole is not selected as an optimal solution. If $\|NTF(e^{j\omega})\|_\infty < 1.5$ which is Lee's rule of thumb for stability, then the cost function minimizes the IBG, subject to the constraint that all poles lie within the unit circle. If $\|NTF(e^{j\omega})\|_\infty \geq 1.5$, the cost function minimizes the weighted in-band gain, $DR*DRFactor$, and the infinity norm subject to the constraint that all poles lie within the unit circle. The factor of 100 weights the IBG so that its weight in the cost function is similar to the weight of $\|NTF(e^{j\omega})\|_\infty$. Note that if $\|H\|_\infty$ is within the maximum value for stability and the poles are all within the unit circle, then the cost function is simply the $IBG + DR*DRFactor$.

3.2 Delsig Designs

In [2], Schreier suggests a method for generating DSM NTFs that are optimal in the SQNR sense. The NTF's optimal zeros are determined by minimizing the NTF's power over the frequencies of interest with respect to the NTF's zeros. The poles are then

Reproduced with permission of the copyright owner. Further reproduction prohibited without permission.

found iteratively. The resulting solution is optimal only if the effect that the poles have on the NTF is negligible and if the quantization noise is white[19]. Schreier also provides a delta sigma design toolkit for Matlab [2], which uses this method for generating optimized DSMs. The toolbox uses a lookup table, the same as Table 2, and divides this result by the OSR. Once the zero positions have been set via the table, the toolbox finds the poles using an iterative approach. This process only finds maximally flat all-pole transfer functions, which may not be the optimal. Also, the zeros may not be optimal when a value of $\|H\|_\infty$ near 1 is desired [1].

3.2.1 Optimal Bandpass Designs

The design toolkit can create BPDSMs. It does this by first designing a lowpass DSM NTF and then performing the pseudo *N*-path transform $z = -z^2$. Assuming the lowpass NTF is, causal, linear, and time invariant, the resulting NTF has the same stability and gain properties as the original NTF but is compressed and shifted in the frequency domain. For bandpass DSMs, this design method creates a notch filter NTF shape, which is often unnecessarily restrictive.

Reproduced with permission of the copyright owner. Further reproduction prohibited without permission.

CHAPTER 4

TEST PROCEDURES AND RESULTS

In this chapter, the performance of several simulated single-bit DSMs that were designed using DE and the delsig toolbox are compared with respect to the DSMs' SQNRs and DRs. In particular, the types of DSMs that are compared are LP, VLIF and BP of orders 2-8 and with OSRs of 32, 64, and 128. Several graphs summarize the resultant SQNRs and DRs.

4.1 Design and Test Procedures

Typically, DSMs are designed to a set of specifications such as bandwidth, clock frequency, SQNR, DR and power consumption. These constraints will, in turn, help determine the needed order and OSR needed to satisfy these specifications. In order to maintain generality in this thesis, however, the reverse approach is taken. The DSM order and OSR are chosen at the start of a design. The NTF is then designed to yield the highest SQNR and DR for the given parameters.

Once the NTF is designed, a DSM is constructed by incorporating the NTF into the Boser-Wooley Modulator architecture [20] which has a unity STF magnitude response within the passband. Each DSM is simulated several times in the time domain using the input of a single sine wave of amplitude 0.5 and of various frequencies within the

Reproduced with permission of the copyright owner. Further reproduction prohibited without permission.

passband. The results are then windowed using a Chebyshev window. A Fast Fourier Transform (FFT) is then used to produce the spectral information.

The spectra resulting from the FFT is used to determine the DSM's SQNR, DR and stability. The SQNR is determined by finding the ratio of the average signal power to the average noise power of the DSM. The dynamic range is defined as the ratio of the largest to smallest signals that a DSM can resolve within the passband. The simulated power spectral density (PSD) is also used to determine the stability of a DSM. The PSD of a stable DSM will closely match the prediction of its linear model. Furthermore, if a DSM is unstable, the time domain simulations will show SQNRs and DRs that are significantly worse than those predicted by the linear model.

The remaining sections of this chapter compare the results of several DSMs designed using the DE algorithm with the results of comparable DSMs designed using the delsig toolbox. These results are organized by the DSM's passband requirements i.e., lowpass, bandpass, and very low IF. For each of these cases, a comparison of the linear models for two of the DSMs is presented, as well as a comparison of the PSD of the time domain simulation and the corresponding linear model prediction. Since the STF is always unity in the passband, only the DSM NTFs are shown. Following these examples are graphs comparing the time simulated DR and SQNR for 2nd through 8th order DSMs that were designed using DE and the delsig toolbox.

4.2 Low Pass DSM Results

Lowpass DSMs include the zero frequency in their passband. All NTFs were designed by first selecting the order and OSR, and then optimizing for the lowest SQNR

Reproduced with permission of the copyright owner. Further reproduction prohibited without permission.

and DR. All frequencies shown are normalized to 2π radians / sample = 1. Because of this, all passband bandwidths are a function of the OSR and can be calculated as 0.5 / OSR radians (rad) per sample.

An exhaustive set of spectra plots for all the DSMs simulated in this section would be too numerous to include, so only the spectrum plots for the 2nd order LPDSM with an OSR 128 and the 8th order LPDSM with an OSR of 32 are shown. Concluding this section are three plots that summarize the time domain simulation results for 2nd through 8th order LPDSMs that have OSRs of 32, 64, and 128 and were designed using DE and the delsig toolbox.

4.2.1 Results for Second Order LPDSM

Figure 18 shows two linearly modeled 2nd order DSM NTFs over the DSMs' passbands. The DSMs were designed with an OSR of 128 which yields a normalized bandwidth of 0.0039π rad/sample. The solid line is the NTF generated by delsig, while the dashed line is the NTF found using differential evolution. As shown in Figure 18, the NTF determined using DE has more noise suppression than the NTF found using delsig.

Figure 19 compares the linearly modeled NTF and the PSD of the 2nd order lowpass DSM designed using DE. The figure shows that the noise spectrum closely matches the linear model, and that the DSM is stable.

Reproduced with permission of the copyright owner. Further reproduction prohibited without permission.

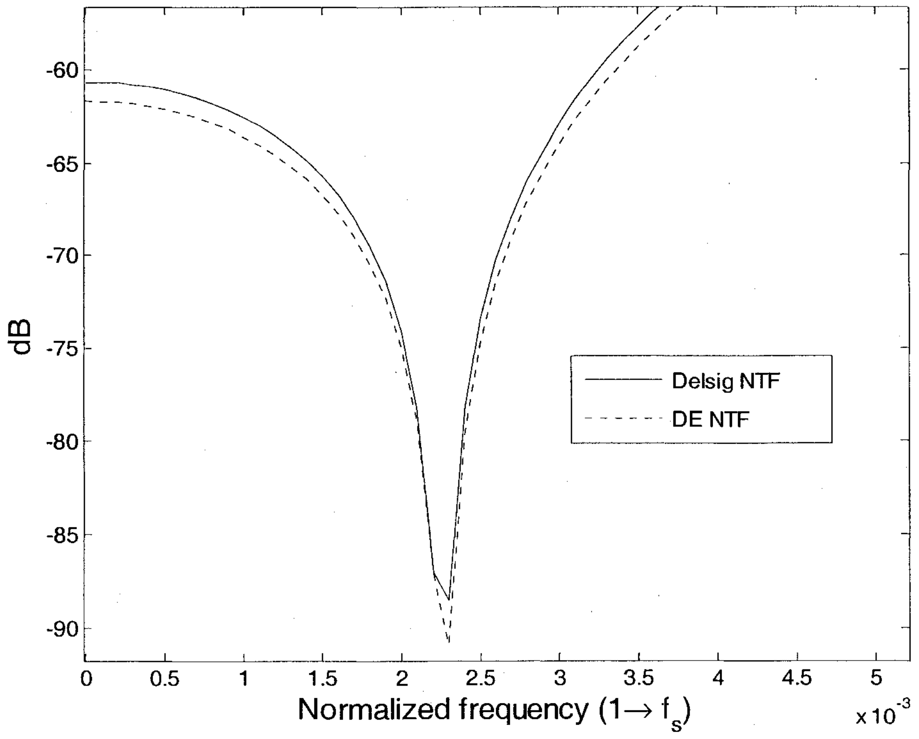

Figure 18: 2^{nd} order lowpass DSM NTFs generated using DE and the delsig toolbox. The NTFs were designed for a LPDSM that has an OSR of 128 and a passband of 0.004π rad/sample.

Reproduced with permission of the copyright owner. Further reproduction prohibited without permission.

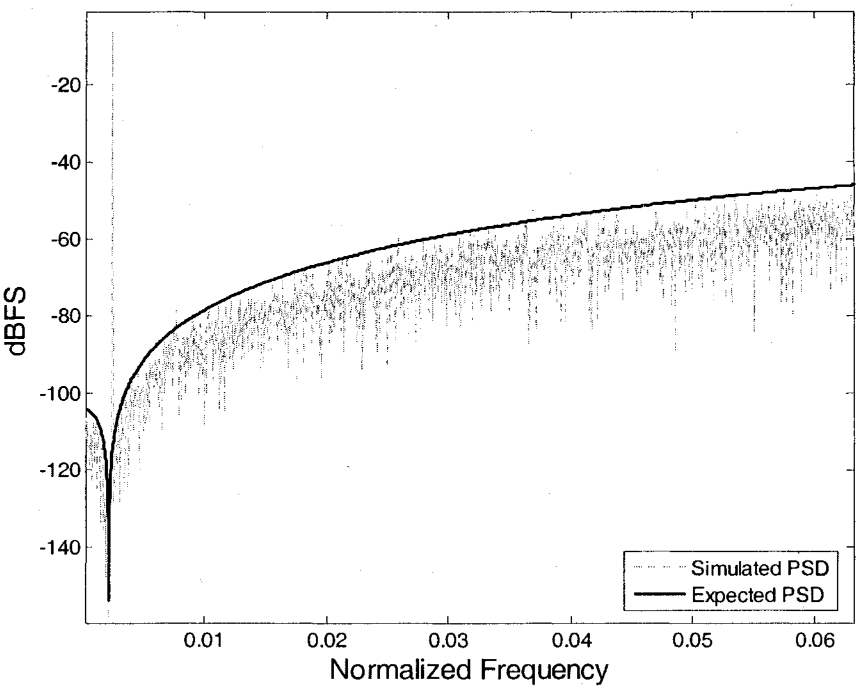

Figure 19: PSD simulation of 2nd order DSM NTF generated using DE.
The NTF was designed for a LPDSM that has an OSR of 128
and a passband of 0.004π rad/sample.

4.2.2 Results for an Eight Order LPDSM

Figure 20 shows two 8th order DSM NTFs over the DSMs' passbands. The DSMs were designed with an OSR of 32 which yields a normalized bandwidth of 0.016π rad/sample. The solid line is the NTF generated by delsig, while the dashed line is the NTF found using differential evolution. As shown in Figure 20, the NTF determined using DE has more noise suppression than the NTF found using delsig.

Reproduced with permission of the copyright owner. Further reproduction prohibited without permission.

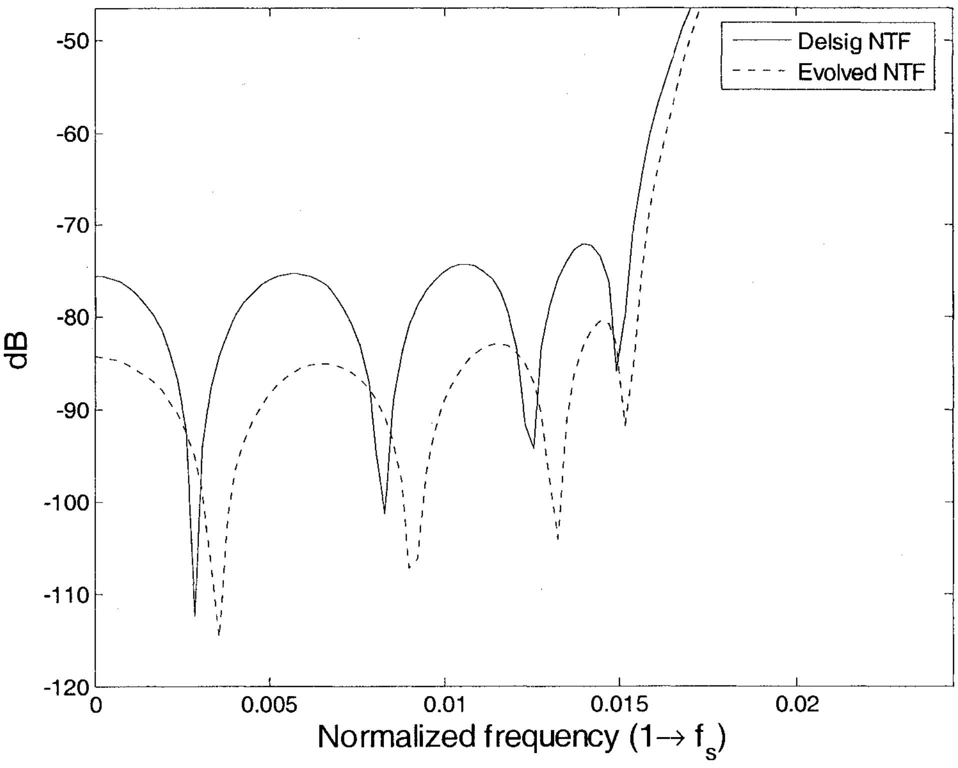

Figure 20: 8th order lowpass DSM NTFs generated using DE and the delsig toolbox. The NTFs were designed for a LPDSM that has an OSR of 32 and a passband of 0.016π rad/sample.

Reproduced with permission of the copyright owner. Further reproduction prohibited without permission.

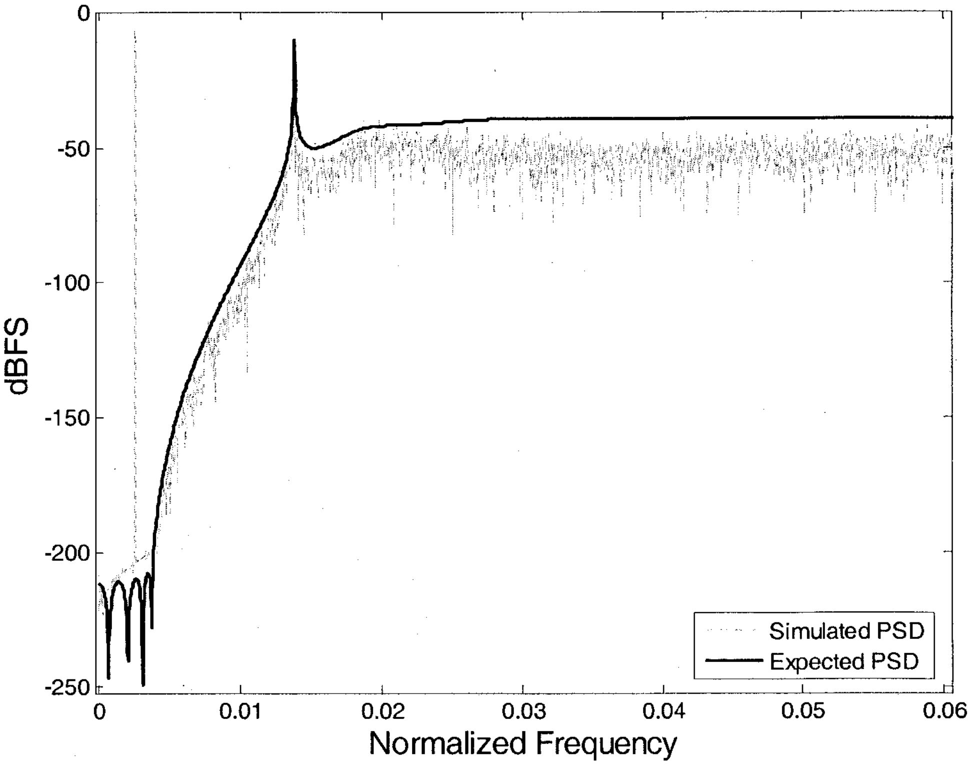

Figure 21: PSD Simulation of 8th order NTF Generated using DE.
The NTF was designed for a LPDSM that has an OSR of 32
and a passband of 0.016π rad/sample.

Figure 21 compares the linearly modeled NTF and the PSD of the 8th order lowpass DSM designed using DE. The figure shows that the noise spectrum closely matches the linear model, and that the DSM is stable. The out of band gain for this DSM is above the threshold suggested for Lee's rule. This high Q pole reduces the noise in the passband with no effect on the stability of the DSM.

4.2.3 Comparison of DR and SQNR for Delsig and DE LPDSM NTFs

Figure 22, Figure 23 and Figure 24 compare the SQNRs and DRs for 2nd through 8th order lowpass DSMs with an OSR of 32, 64, and 128, respectively. As shown in the

Reproduced with permission of the copyright owner. Further reproduction prohibited without permission.

figures, the DE generated DSMs have higher SQNRs and DRs than the DSMs designed using delsig. In the figures, if can be seen that the 8th order DSMs often performed worse than the 7th order DSMs. This degradation in performance is to due higher order DSMs requiring a lower infinity norm of 1.4 to remain stable. This lower infinity norm caused a decrease in performance relative to the 7th order DSM. This is especially apparent in the delsig designed DSMs.

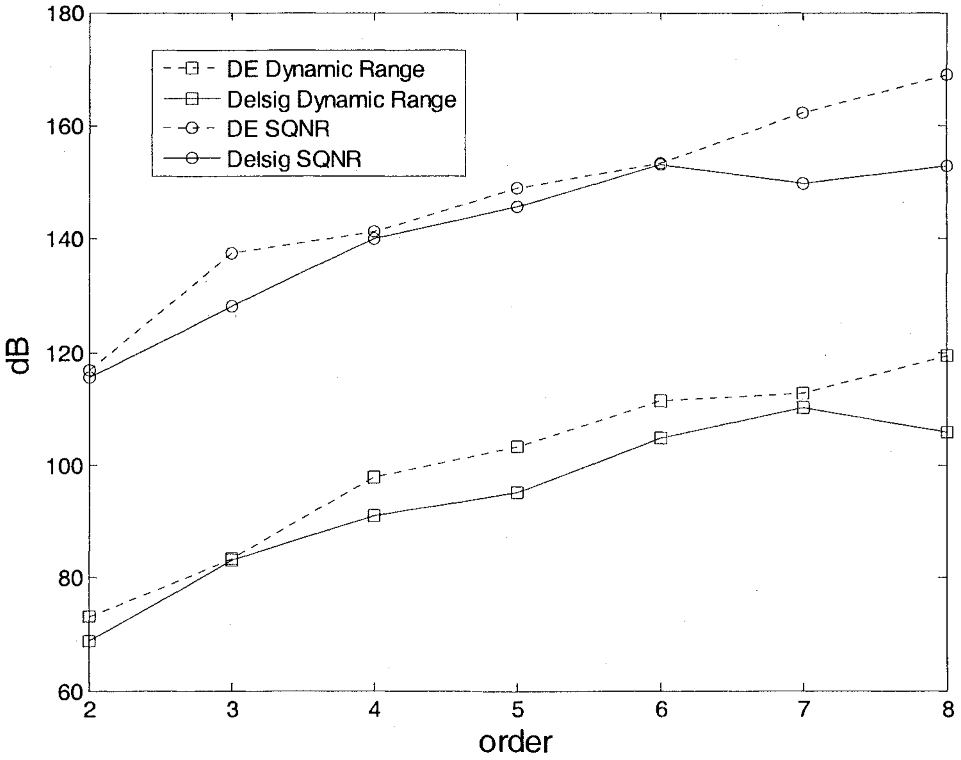

Figure 22: SQNR and DR results for lowpass DSMs with OSR = 32, $f_0 = 0$ and a bandwidth of 0.016π rad/sample.

Reproduced with permission of the copyright owner. Further reproduction prohibited without permission.

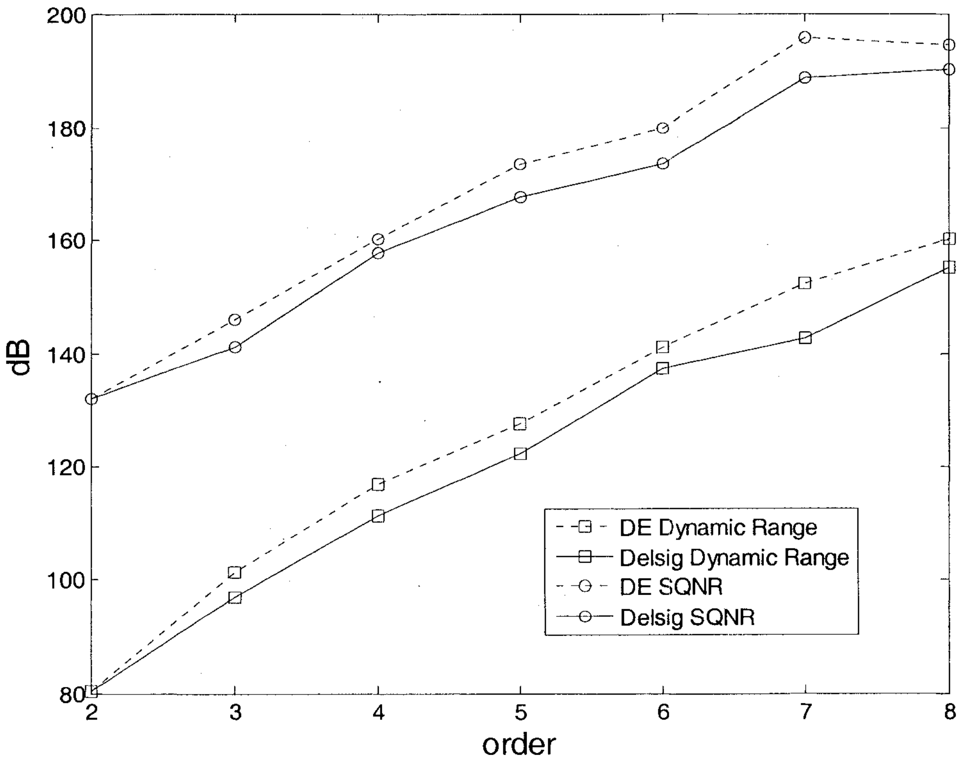

Figure 23: SQNR and DR results for lowpass DSMs with OSR = 64, $f_0 = 0$, and a bandwidth of .008π rad/sample.

Reproduced with permission of the copyright owner. Further reproduction prohibited without permission.

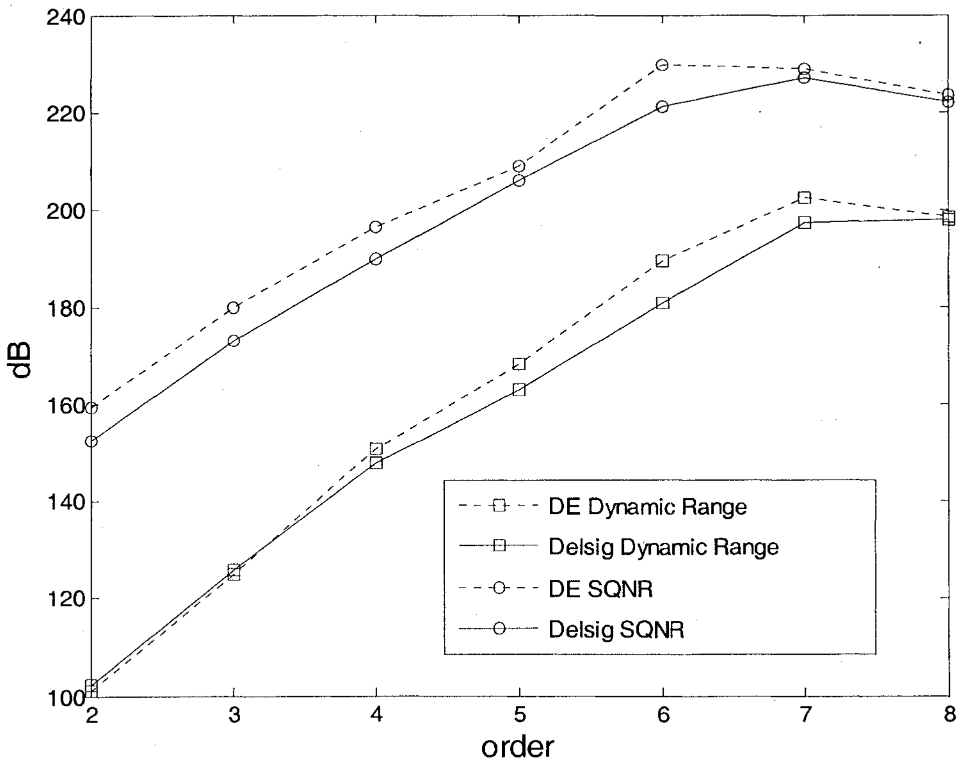

Figure 24: SQNR and DR results for lowpass DSMs with OSR = 128, $f_0 = 0$, and a bandwidth of 0.004π rad / sample.

4.3 VLIF DSM Results

VLIF DSMs have a center frequency very close to zero. All VLIF DSM NTFs were designed by first selecting the order and OSR, and then optimizing for the lowest SQNR and DR. All frequencies shown are normalized to 2π radians / sample = 1. Because of this, all passband bandwidths are a function of the OSR and can be calculated as 0.5 / OSR radians per sample. A normalized center frequency of 0.02 radians / sample was chosen as the center frequency. An exhaustive set of spectra plots for all the DSMs simulated in this section would be too numerous to include, so only spectrum plots for the 2nd order VLIF DSM with an OSR 128 and the 4th order VLIF DSM with an OSR of 64

Reproduced with permission of the copyright owner. Further reproduction prohibited without permission.

are shown. Concluding this section are three plots that summarize the time domain simulation results for VLIF DSMs with even orders 2 through 8 that have OSRs of 32, 64, and 128 and were designed using DE and the delsig toolbox.

4.3.1 Analysis of Second order VLIF DSM

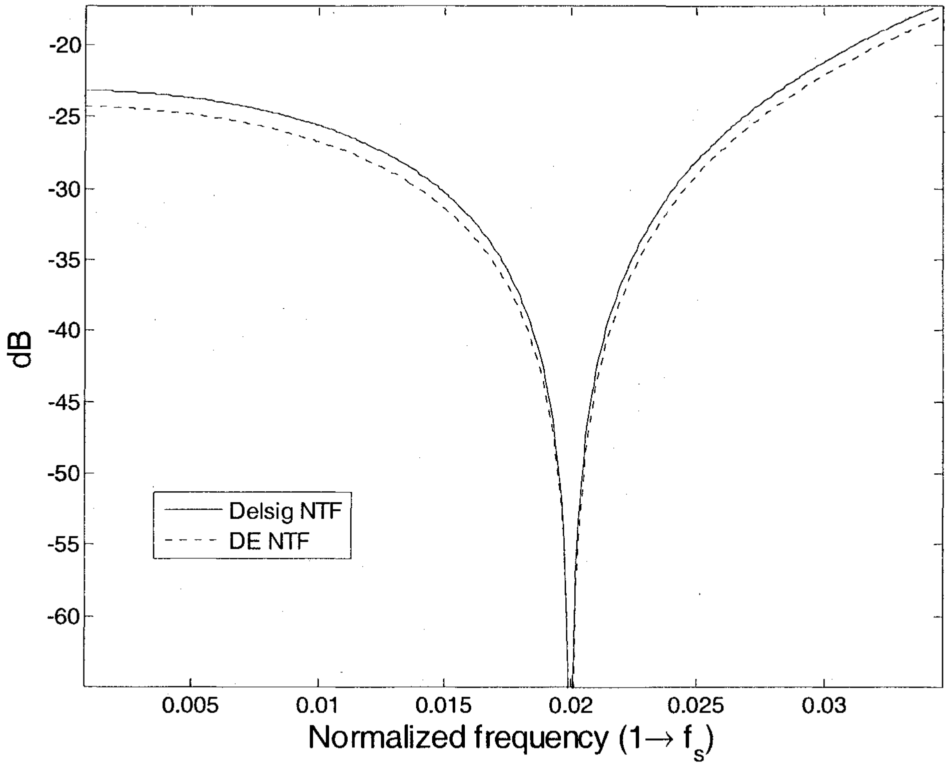

Figure 25: 2nd order NTFs generated using DE and the delsig toolbox. The NTFs were designed for a VLIF DSM that has an OSR of 128, an f_0 of 0.02π rad/sample, and a passband of 0.004π rad/sample.

Figure 25 shows two linearly modeled 2nd order DSM NTFs over the DSMs' passbands. The DSMs were designed with an OSR of 128 which yields a normalized bandwidth of 0.004π rad/sample. The solid line is the NTF generated by delsig, while the

Reproduced with permission of the copyright owner. Further reproduction prohibited without permission.

dashed line is the NTF found using differential evolution. As shown in Figure 25, the NTF determined using DE has more noise suppression than the NTF found using delsig.

Figure 26 compares the linearly modeled NTF and the PSD of the 2nd order VLIF DSM designed using DE. The figure shows that the noise spectrum closely matches the linear model, and that the DSM is stable.

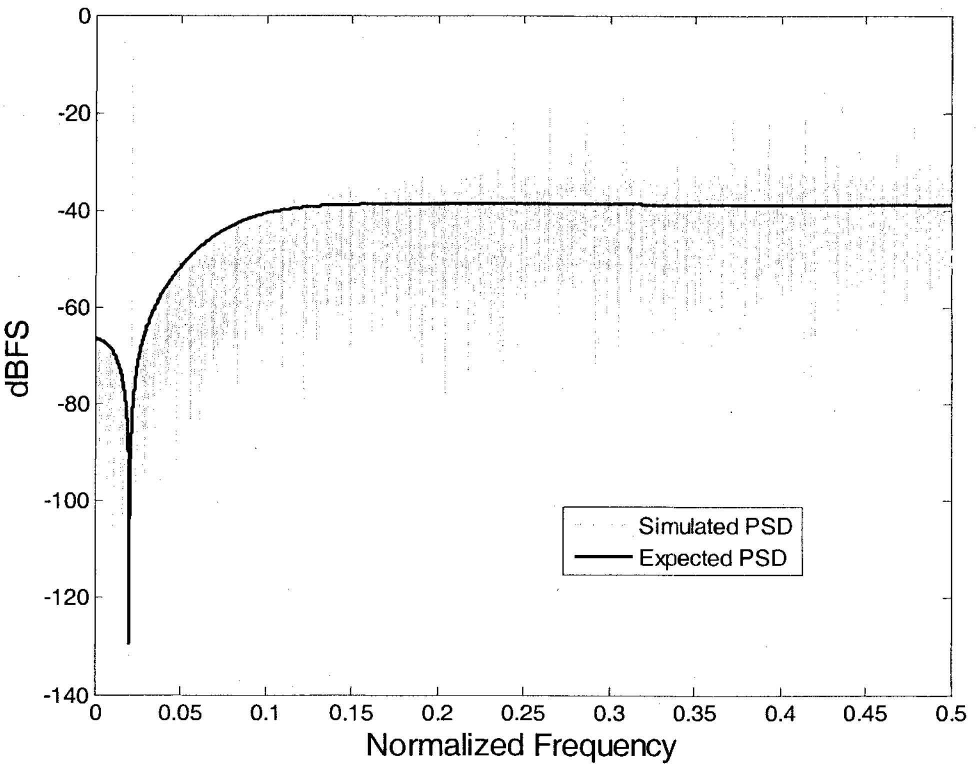

Figure 26: PSD simulation of 2nd order NTF generated using DE. The NTF was designed for a VLIF DSM that has an OSR of 128, an f_0 of 0.02π rad/sample and a passband of 0.004π rad/sample.

4.3.2 Comparison of fourth order VLIF DSM

Figure 27 shows two linearly modeled 4th order DSM NTFs over the DSMs' passbands. The DSMs were designed with an OSR of 64 which yields a normalized

Reproduced with permission of the copyright owner. Further reproduction prohibited without permission.

bandwidth of 0.008π rad/sample. The solid line is the NTF generated by delsig, while the dashed line is the NTF found using differential evolution. As shown in Figure 27, the NTF determined using DE has more noise suppression than the NTF found using delsig. This is due to, in part, the ability of DE to design an NTF with a steeper response in the out of band signal.

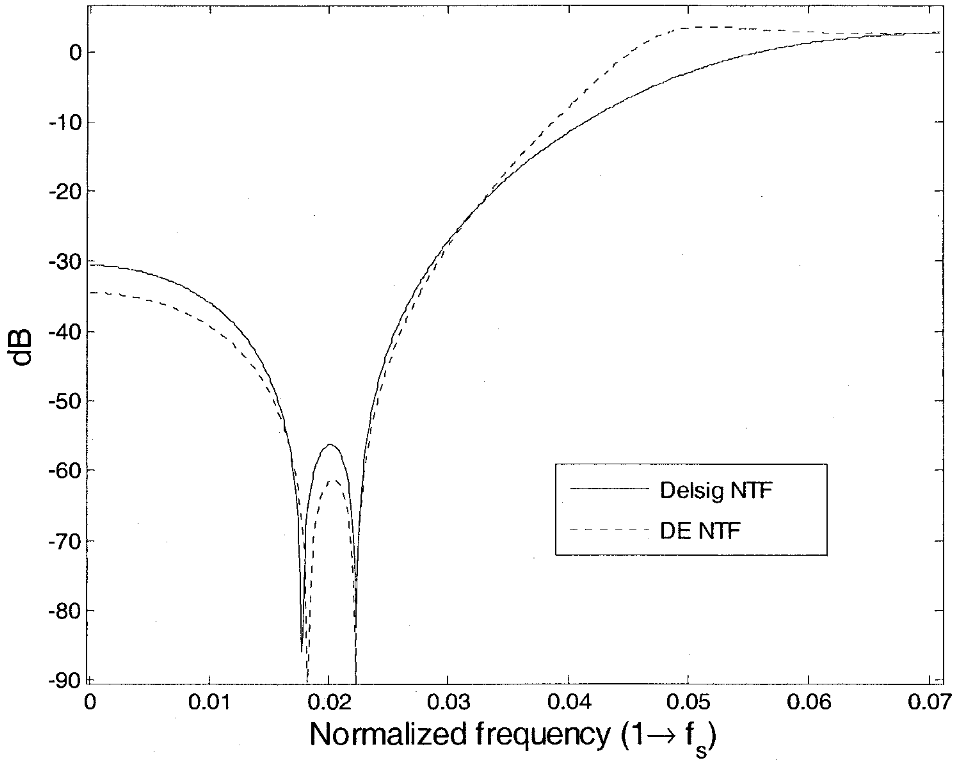

Figure 27: 4th order NTFs generated using DE and the delsig toolbox. The NTFs were designed for a VLIF DSM that has an OSR of 64, a f_0 of 0.02π rad/sample, and a passband of 0.008π rad/sample.

Reproduced with permission of the copyright owner. Further reproduction prohibited without permission.

Figure 28 shows that this increase in out of band gain does not affect the stability of the system because the noise suppression within the passband closely matches the PSD predicted by the linear model.

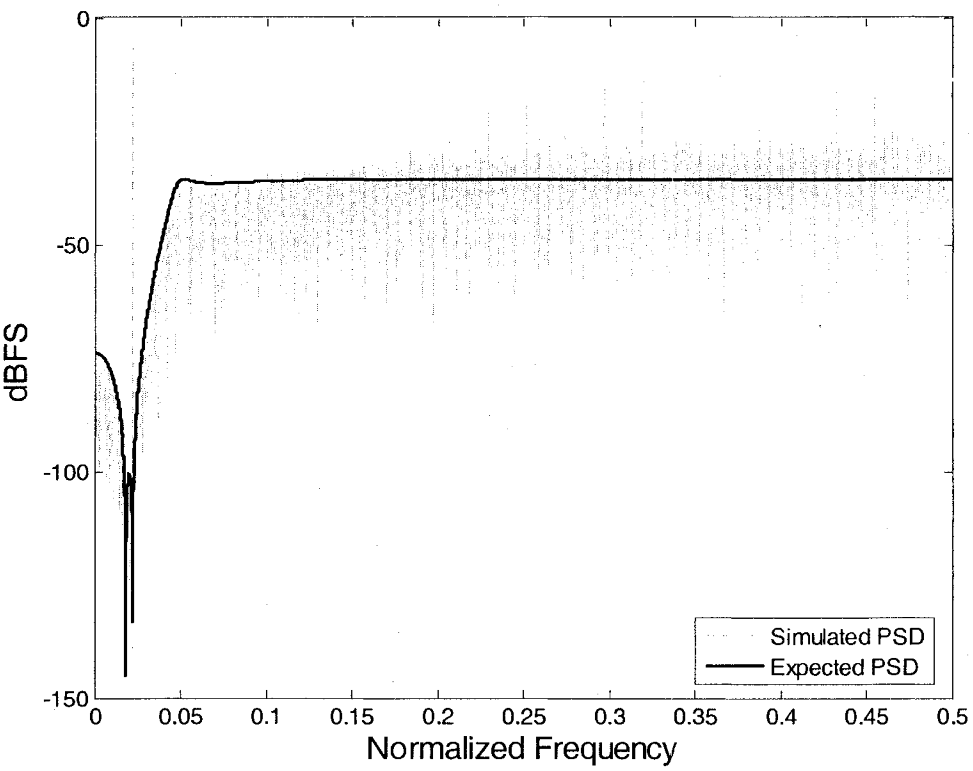

Figure 28: PSD Simulation of 4th order NTF generated using DE. The NTF was designed for a VLIF DSM that has an OSR of 64, an f_0 of 0.02π rad/sample, and a passband of 0.008π rad/sample.

4.3.3 Comparison of DR and SQNR for Delsig and DE VLIF DSM NTFs

Figure 29, Figure 30, and Figure 31 compare of the SQNR and DR for VLIF DSMs with OSRs of 32, 64 and 128 respectively. Even orders of 2 through 8 are simulated with a normalized center frequency of 0.02π radians. The DSMs designed using DE always has better SQNRs and DRs than the corresponding DSMs designed

Reproduced with permission of the copyright owner. Further reproduction prohibited without permission.

using delsig. The DE DSMs did especially well in comparison to the 8th order delsig DSMs.

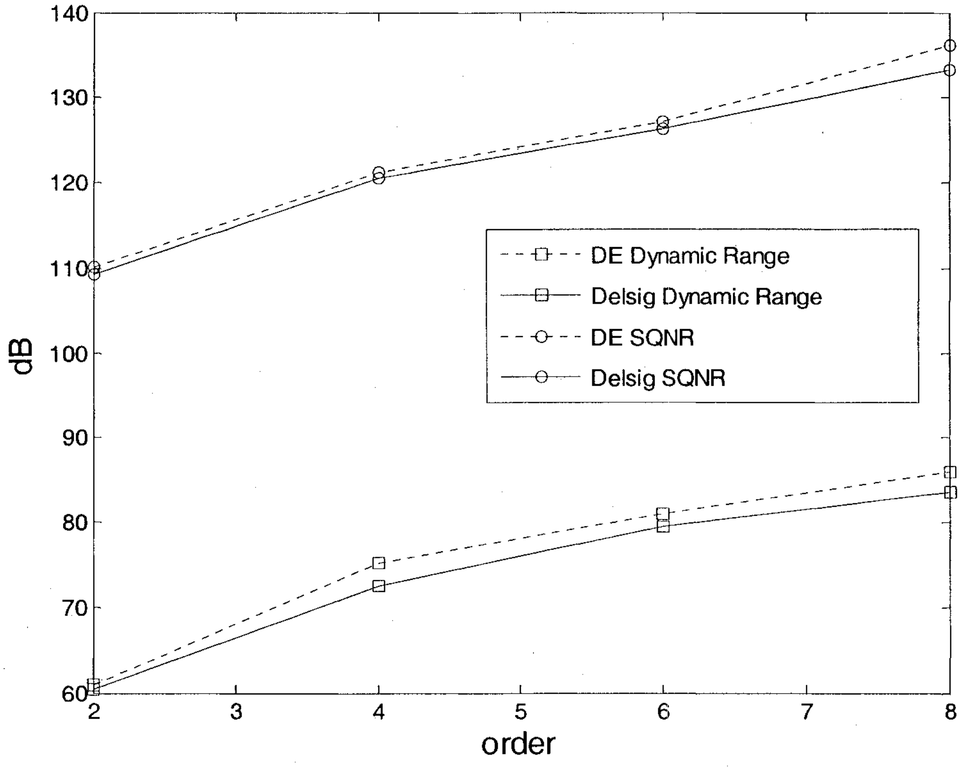

Figure 29: SQNR and DR results for VLIF DSMs with OSR = 32, $f_0 = 0.02\pi$ rad/ sample, and a bandwidth of 0.016π rad / sample.

Reproduced with permission of the copyright owner. Further reproduction prohibited without permission.

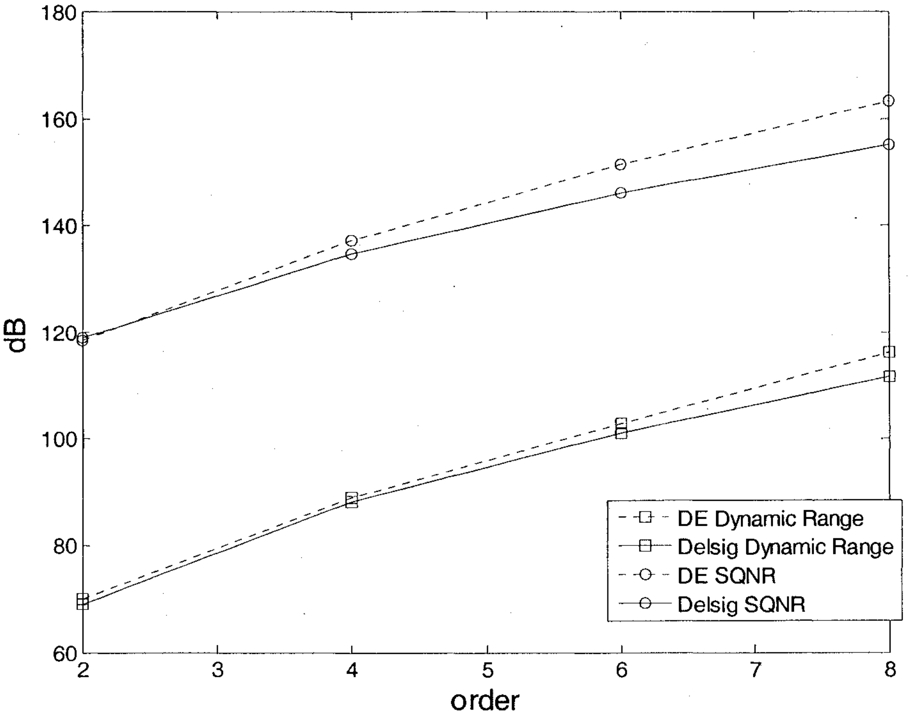

Figure 30: SQNR and DR results for VLIF DSMs with OSR = 64, $f_0 = 0.02\pi$ rad/ sample, and a bandwidth of 0.008π rad / sample.

Reproduced with permission of the copyright owner. Further reproduction prohibited without permission.

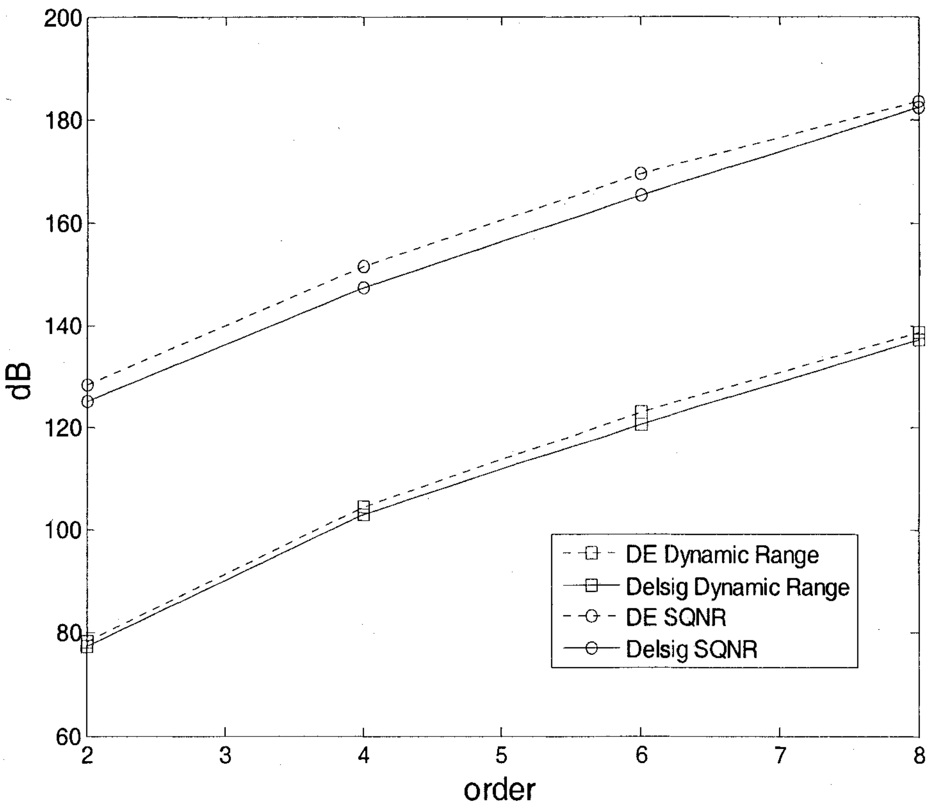

Figure 31: SQNR and DR results for VLIF DSMs with OSR = 128, $f_0 = 0.02\pi$ rad/ sample, and a bandwidth of 0.004π rad / sample.

4.4 Bandpass DSMs

Bandpass DSMs have a center frequency well above zero. All bandpass NTFs were designed by first selecting the order and OSR, and then optimizing for the lowest SQNR and DR. All frequencies shown are normalized to 2π radians / sample = 1. Because of this, all passband bandwidths are a function of the OSR and can be calculated as 0.5 / OSR radians per sample. A normalized center frequency of 0.125π radians / sample was chosen as the center frequency.

Reproduced with permission of the copyright owner. Further reproduction prohibited without permission.

An exhaustive set of spectra plots for all the DSMs simulated in this section would be too numerous to include, so only a 4th order bandpass DSM of OSR 32 is shown. Concluding this section are three plots that summarize the time domain simulation results for 2nd, 4th, 6th, and 8th order bandpass DSMs that have OSRs of 32, 64, and 128 were designed using both DE and the delsig toolbox.

4.4.1 Comparison of Fourth Order BPDSM

Figure 32 shows two linearly modeled 4th order DSM NTFs over the DSMs' passbands.

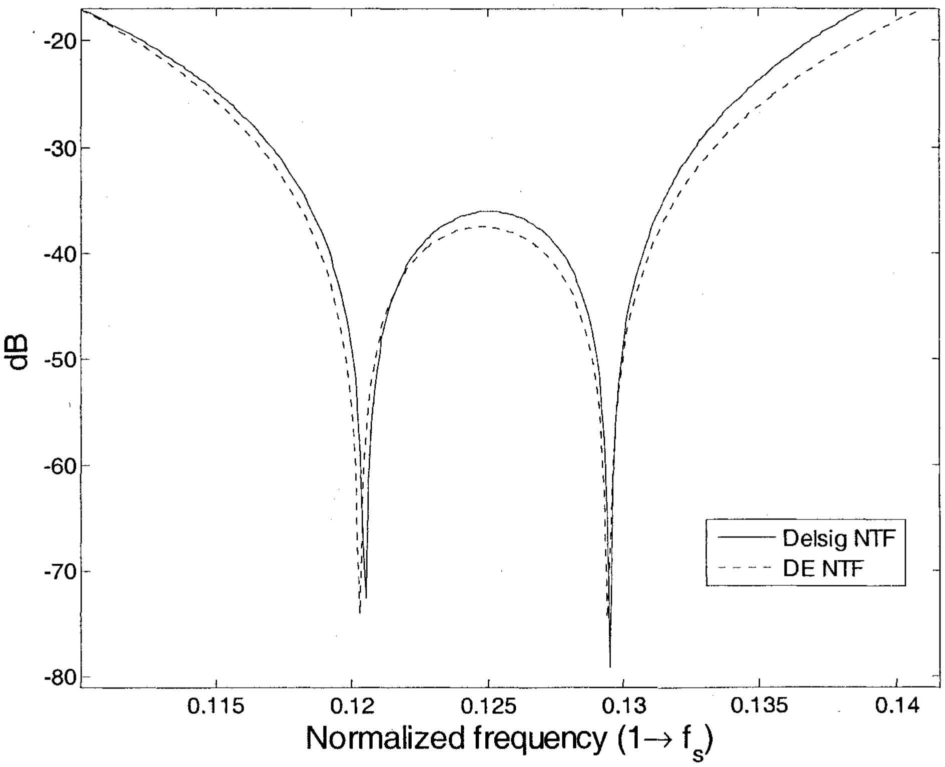

Figure 32: 4th order NTFs generated using DE and the delsig toolbox. The NTFs were designed for a bandpass DSM that has an OSR of 32, an f_0 of 0.125π rad/sample, and a passband of 0.016π rad/sample.

Reproduced with permission of the copyright owner. Further reproduction prohibited without permission.

The DSMs were designed with an OSR of 32 which yields a normalized bandwidth of 0.016π rad/sample. The solid line is the NTF generated by delsig, while the dashed line is the NTF found using differential evolution. As shown in Figure 32, the NTF determined using DE has more noise suppression than the NTF found using delsig. Figure 33 shows that the time domain simulated PSD closely matches the PSD predicted by the linear model within the passband.

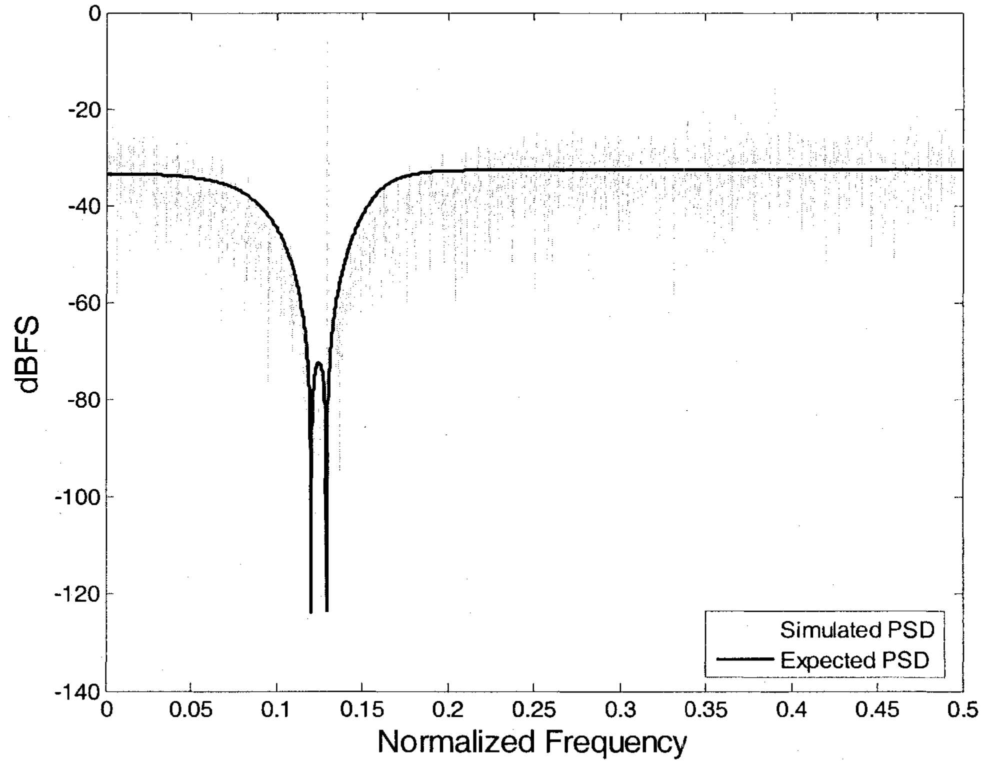

Figure 33: PSD simulation of 4th order NTF generated using DE. The NTF was designed for a VLIF DSM that has an OSR of 64, an f_0 of 0.125π rad/sample, and a passband of 0.016π rad/sample.

Reproduced with permission of the copyright owner. Further reproduction prohibited without permission.

4.4.2 Comparison of DR and SQNR for Delsig and DE BPDSM NTFs

Figure 34, Figure 35, and Figure 36 compare the SQNRs and DRs of 2nd, 4th, 6th and 8th order bandpass DSMs with OSRs of 32, 64 and 128 respectively. All DSMs were simulated with a normalized center frequency of 0.125π radians, and the DSMs designed using DE always had better SQNRs and DRs than the corresponding DSMs designed using delsig.

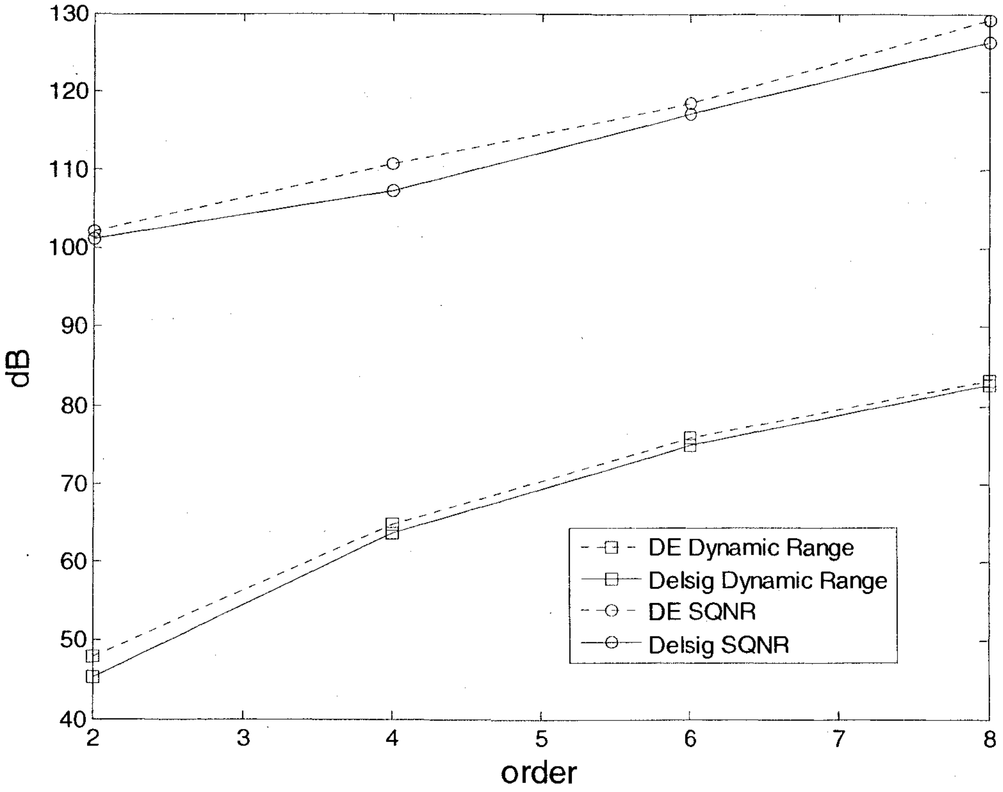

Figure 34: SQNR and DR results for bandpass DSMs with OSR = 32, f_0 = 0.125π rad / sample, and a bandwidth of 0.004π rad / sample.

Reproduced with permission of the copyright owner. Further reproduction prohibited without permission.

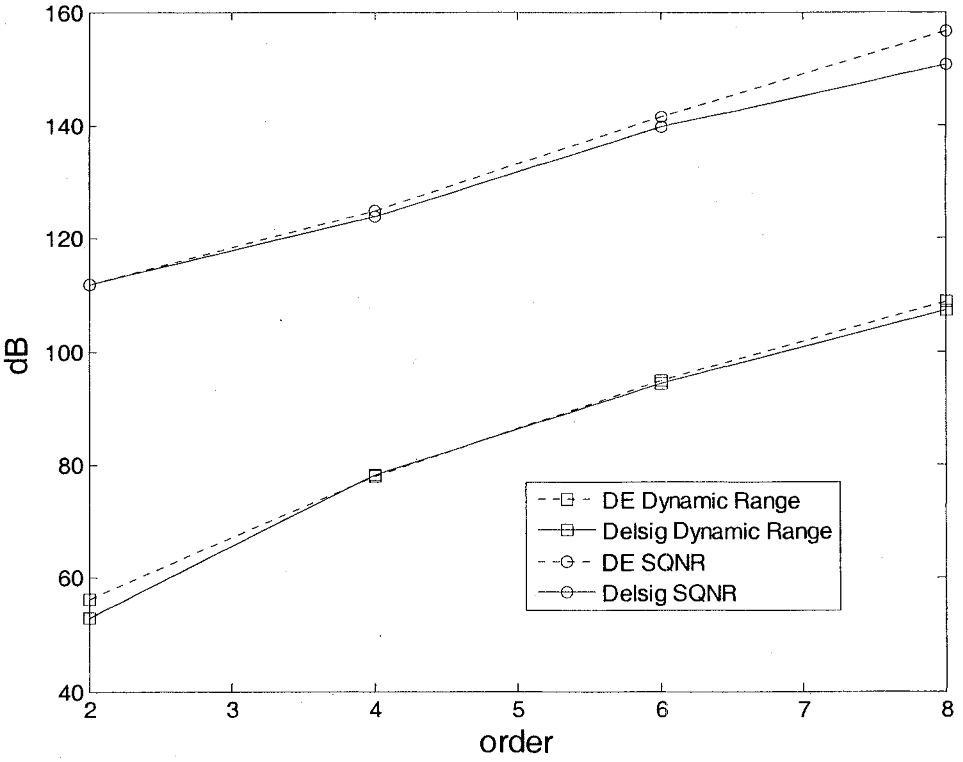

Figure 35: SQNR and DR results for bandpass DSMs with OSR = 64, $f_0 = 0.125\pi$ rad/sample, and a bandwidth of 0.008π rad / sample.

Reproduced with permission of the copyright owner. Further reproduction prohibited without permission.

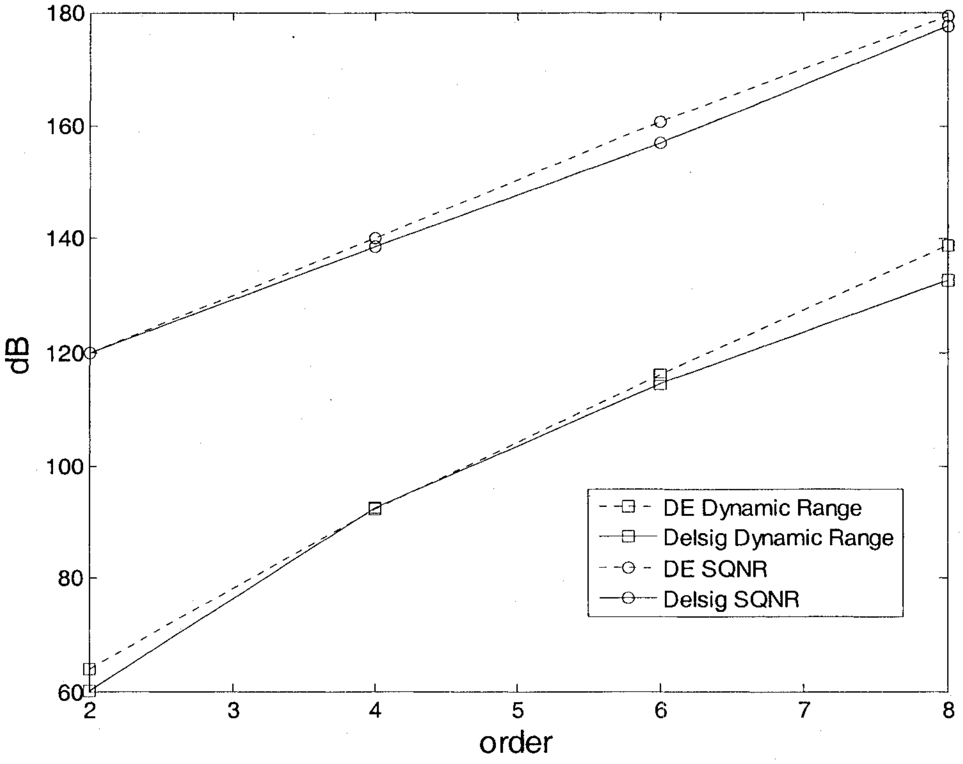

Figure 36: SQNR and DR results for bandpass DSMs with OSR = 128, $f_0 = 0.125\pi$ rad / sample, and a bandwidth of 0.016π rad / sample.

Reproduced with permission of the copyright owner. Further reproduction prohibited without permission.

CHAPTER 5

SUMMARY AND CONCLUSIONS

DSMs are widely used in modern communications systems. They are high performance ADCs that are capable of very high dynamic range DRs and SQNRs; however, designing DSMs is difficult because they are non-linear and require several assumptions and estimates to design using analytic techniques. In this thesis, a GA based on DE is used to generate DSM NTFs. The NTFs were then used to design DSMs and compared to DSMs designed using the delsig matlab toolbox.

The design method developed in thesis is based on a GA called DE, which was developed by Rainer Storn. The algorithm is flexible and allows for optimization of complex objective functions. In the author's experience, it always converged and typically produced a linearized model that outperformed one designed using the delsig toolbox. For the work in this thesis, DE proved to be an effective method for designing DSMs. The method is easy to use and lends itself to modification for specific requirements. Additionally, the DE algorithm used in this thesis relaxed the NTF out of band gain requirements with no loss in stability. Further research on this effect could prove useful.

The main disadvantage of this method is common to all DSM methods; there isn't a quick and reliable calculation to determine the stability of a DSM. This makes

Reproduced with permission of the copyright owner. Further reproduction prohibited without permission.

optimization for stability impossible, which in turn requires designs to be conservative in their out of band gain requirements. Additionally, DE typically converges relatively slowly when compared to other techniques. The algorithm developed in this thesis, however, can be seeded with variations around an already "near optimal" NTF. This can greatly reduce computation time by reducing the solution space.

Not only did the linear models of the DE designed NTFs predict better noise suppression than those designed using delsig, but time domain simulation confirmed that DSMs designed using DE typically produced DSMs with 1%~10% better SQNRs and DRs than those found using the delsig toolbox. Moreover, higher order DSMs typically benefited more from the DE because it becomes more important to optimize the poles and zeros at the same time, which the iterative approach used by delsig does not do. Thus DE can design lowpass, bandpass, and very low intermediate frequency DSMs that have better performance metrics than currently used design techniques.

Reproduced with permission of the copyright owner. Further reproduction prohibited without permission.

REFERENCES

[1] Storn, R. and Price, K., *Differential Evolution - a Simple and Efficient Adaptive Scheme for Global Optimization over Continuous Spaces*, Technical Report TR-95-012, ICSI, March 1995, ftp.icsi.berkeley.edu.

[2] Schreier, Richard; Temes, Gabor C., *Understanding Delta-Sigma Data Converters*, Piscataway, NJ, John-Wiley and Sons, Inc., 2005.

[3] http://en.wikipedia.org/wiki/Tuned_radio_frequency_receiver, June 2005

[4] Storn, R., *Differential Evolution Design of an IIR-Filter with Requirements for Magnitude and Group Delay,* Technical Report TR-95-026, ICSI, June 1995, ftp.icsi.berkeley.edu.

[5] Storn, R., *FiWiz software program*, http://www.icsi.berkeley.edu/~storn/fiwiz.html

[6] Lyons, Richard, *Quadrature Signals: Complex, But Not Complicated*, www.dspguru.com/info/tutor/quadsig2.htm

[7] Hoeschele, David F., *Analog-to-digital and Digital-to-Analog conversion techniques*, 2nd edition, New York, NY, John-Wiley and Sons, Inc., 1994.

[8] Beis, Uwe, *An Introduction to Delta Sigma Converters,* http://www.beis.de/Elektronik/DeltaSigma/DeltaSigma.html

[9] W.L. Lee, *A novel higher order interpolative modulator topology for high resolution oversampling A/D converters*, Master's Thesis, Massachusetts Institute of Technology, Cambridge, MA, June 1987

[10] K.C.H Chao, S. Nadeem, W.L. Lee, and C.G. Sodini, *A higher order topology for interpolative modulators for oversampling A/D converters*, IEEE Transactions on Circuits and Systems, vol. 37, pp 309-318, March 1990.

[11] Norsworth, Steven R., Schreier, Richard and Temes, Gabor C., *Delta Sigma Data Converters, Theory Design and Simulation*, Piscataway, NJ, Institute of Electrical and Electronic Engineers Press, 1997

Reproduced with permission of the copyright owner. Further reproduction prohibited without permission.

[12] Dileepan Joseph, Lionel Taranssenko and Steve Collins, *Analysis and Simulation of a Cascaded Delta Delta-Sigma Modulator*, Advanced A/D and D/A Conversion Techniques and their Applications, Publication No. 466, July 1999.

[13] J. Steensgaard, *High-Performance Data Converters*, Ph.D. dissertations, Technical University of Denmark, Dept. of Information Technology, pp. 170-171, March 8, 1999.

[14] J. Silva, U. Moon, K. Steensgaard, and G.C. Temes, *Wideband low-distortion delta-sigma ADC topology*. IEE Electronic Letters, vol. 37, no. 12, pp 737-738, June 7, 2001

[15] P. Benabes, A. Gauthier and D. Billet, *New wideband sigma-delta convertor*, IEE Electronic Letters, vol. 29, no 17, pp. 1575-1577, August 19, 1993

[16] Widrow, Bernard; Stearns, Samuel D., *Adaptive Signal Processing*, Upper Saddle River, NJ, Prentice-Hall, Inc,. 1985

[17] Widrow, Bernard; Titchener, Paul F.; Gooch, Richard P. *Adaptive Design of Digital Filters*, Information Systems Laboratory, Stanford University, 1981

[18] http://www.cs.cmu.edu/Groups/AI/html/faqs/ai/genetic/top.html

[19] R. Schreier, *An empirical study of high-order single-bit delta-sigma modulators*, IEEE Transactions on Circuits and Systems II, vol. 40, no.8, pp 461-466, August 1993

[20] B. E. Boser and B. A. Wooley, *The design of sigma-delta modulation analog-to-digital converters*, IEEE Journal of Solid-State Circuits, vol. 23, pp. 1298-1308, December 1988

Reproduced with permission of the copyright owner. Further reproduction prohibited without permission.

VITA

Graduate College
University of Nevada, Las Vegas

Gregory K. Lull

Local Address:
1477 Unionville Lane
Las Vegas, Nevada 89110

Home Address:
6400 Lonas Dr.
Apt # 315
Knoxville, TN 37909

Degrees:
Bachelor of Science, Electrical Engineering, 2002
University of Nevada, Las Vegas

Thesis Title: Adaptive Design of Delta Sigma Modulators

Thesis Examination Committee:
Chairperson, Professor, Dr. Peter Stubberud, Ph.D.
Committee Member, Professor, Dr. Yahia Bagzous, Ph.D.
Committee Member, Professor, Dr. Sahjendra Singh, Ph.D.
Committee Member, Professor, Dr. Brendan O'Toole, Ph.D.

Reproduced with permission of the copyright owner. Further reproduction prohibited without permission.